Balanced activity of multiple FtsW and RodA proteins is crucial for maintaining cell shape and antibiotic resistance in *Listeria monocytogenes*

Jeanine Rismondo[1], Sven Halbedel[2] and Angelika Gründling[1#]

[1] Section of Microbiology and Medical Research Council Centre for Molecular Bacteriology and Infection, Imperial College London, London SW7 2AZ.

[2] FG11 Division of Enteropathogenic bacteria and *Legionella*, Robert Koch-Institute, Burgstrasse 37, 38855 Wernigerode, Germany.

[#]To whom correspondence should be addressed: Angelika Gründling – a.grundling@imperial.ac.uk

Abstract word count: 247

Main text word count: 5957

Running Title: Functional analysis of multiple SEDS in *Listeria*

Abstract

Rod-shaped bacteria have two modes of peptidoglycan synthesis: lateral synthesis and synthesis at the cell division site. These two processes are controlled by two macromolecular protein complexes, the Rod complex and divisome, respectively. Recently, it has been shown that the *Bacillus subtilis* RodA protein, which forms part of the Rod complex, has peptidoglycan glycosyltransferase activity. The cell division specific RodA homolog FtsW fulfils a similar role at the divisome. The human pathogen *Listeria monocytogenes* encodes up to six FtsW/RodA homologs, however their functions have not yet been investigated. Analysis of deletion and depletion strains led to the identification of the essential cell division-specific FtsW protein, FtsW1. Interestingly, *L. monocytogenes* encodes a second FtsW protein, FtsW2, which can compensate for the lack of FtsW1, when expressed from an inducible promoter. *L. monocytogenes* also possesses three RodA homologs, RodA1, RodA2 and RodA3 and their combined absence is lethal. Cells of a *rodA1*/*rodA3* double mutant strain are shorter and have increased antibiotic and lysozyme sensitivity, probably due to a weakened cell wall. Results from promoter activity assays revealed that expression of *rodA3* and *ftsW2* is induced in the presence of antibiotics targeting penicillin binding proteins. Consistent with this, a *rodA3* mutant was also more susceptible to the ß-lactam antibiotic cefuroxime. Taken together, our study highlights that *L. monocytogenes* encodes a multitude of functional FtsW and RodA enzymes to produce its rigid cell wall and that their expression needs to be tightly regulated to maintain growth, cell division and antibiotic resistance.

Importance

The human pathogen *Listeria monocytogenes* is usually treated with high doses of ß-lactam antibiotics, often combined with gentamicin. However, these antibiotics only act bacteriostatically on *L. monocytogenes* and the immune system is needed to clear the infection. Therefore, individuals with a compromised immune system are at risk to develop a severe form of *Listeria* infection, which can be fatal in up to 30% of cases. The development of new strategies to treat *Listeria* infections is therefore necessary. Here we show that the expression of some of the FtsW and RodA enzymes of *L. monocytogenes* is induced by the presence of ß-lactam antibiotics and their combined absence makes bacteria more susceptible to this class of antibiotics. The development of antimicrobials that inhibit the activity or production of FtsW/RodA enzymes might therefore help to improve the treatment of *Listeria* infections and thereby lead to a reduction in mortality.

Introduction

Bacterial cells are surrounded by a mesh of peptidoglycan (PG) that determines their shape and also protects the cells from lysis due to their high internal turgor pressure (Weidel and Pelzer, 1964, Vollmer et al., 2008). Peptidoglycan is comprised of glycan strands that are crosslinked by short peptides (Rogers et al., 1980). The glycan strands are composed of alternating N-acetylglucosamine and N-acetylmuramic acid residues that are connected by a ß-1,4 glycosidic bond (Ghuysen and Strominger, 1963). The synthesis of peptidoglycan begins in the cytoplasm with the production of the PG precursor lipid II by the proteins MurABCDEF, MraY and MurG (Blumberg and Strominger, 1974, van Heijenoort, 2001, Scheffers and Pinho, 2005, Pinho et al., 2013). Lipid II is then transported across the cytoplasmic membrane by the flippase MurJ and Amj (Meeske et al., 2015, Sham et al., 2014, Ruiz, 2008) and subsequently incorporated in the growing glycan strand by glycosyltransferases. The polymerization and the crosslinking of the glycan strands are facilitated by the activity of glycosyltransferases and transpeptidases, respectively. Class A penicillin binding proteins (PBPs) are bifunctional enzymes that possess glycosyltransferase and transpeptidase activity, whereas class B PBPs only contain a transpeptidase domain (Höltje, 1998, Sauvage et al., 2008, Goffin and Ghuysen, 1998). In addition, some species such as *Escherichia coli*, *Staphylococcus aureus* and *Streptococcus pneumoniae* encode monofunctional glycosyltransferases (MGTs) that can also incorporate lipid II into the growing glycan strand (Park and Matsuhashi, 1984, Park et al., 1985, Karinou et al., 2018, Wang et al., 2001, Hara and Suzuki, 1984).

B. subtilis encodes four class A PBPs and no MGT, however, deletion of all class A PBPs only manifests in small PG changes (McPherson and Popham, 2003). Recently, it has been shown that members of the SEDS (shape, elongation, division, sporulation) family of proteins, namely RodA and FtsW, also act as glycosyltransferases (Meeske et al., 2016, Cho et al., 2016, Emami et al., 2017, Taguchi et al., 2019). Both, RodA and FtsW, form

90 complexes with cognate class B PBPs to enable polymerization and crosslinking of glycan
91 strands (Cho et al., 2016, Taguchi et al., 2019, Leclercq et al., 2017, Fraipont et al., 2011).
92 Interestingly, SEDS proteins and the class B PBPs are more conserved among different
93 bacterial species than class A PBPs (Meeske et al., 2016).
94 In rod-shaped bacteria, peptidoglycan is synthesized by two multiprotein complexes, the rod
95 complex that is essential for the cell elongation and the divisome that is crucial for the
96 formation of the division septum (Ricard and Hirota, 1973, Nanninga, 1991, Carballido-
97 Lopez and Formstone, 2007). RodA is part of the rod complex and is essential in many
98 bacteria including *B. subtilis* and *S. pneumoniae* (Liu et al., 2017, Henriques et al., 1998).
99 Depletion of RodA results in the production of enlarged, spherical cells in *B. subtilis*
100 (Henriques et al., 1998). In contrast, FtsW is essential for cell division and cells depleted for
101 FtsW grow as long filaments (Kobayashi et al., 2003, Boyle et al., 1997, Gamba et al., 2016).
102 *B. subtilis* harbors a sporulation specific member of the SEDS family, SpoVE in addition to
103 RodA and FtsW. SpoVE is dispensable for growth, however, it is essential for the synthesis
104 of the spore cortex peptidoglycan (Henriques et al., 1992, Ikeda et al., 1989). Other *Bacillus*
105 species such as *B. cereus* and *B. anthracis* possess 4 to 5 FtsW/RodA proteins and strains of
106 different serotypes of the human pathogen *Listeria monocytogenes* encode even up to 6
107 FtsW/RodA homologs in their genome. However, their functions have not yet been
108 investigated.
109 Here, we determine the role of the different FtsW and RodA homologs for the growth and
110 cell morphology of *L. monocytogenes*. Our results show that *L. monocytogenes* encodes two
111 FtsW and three RodA enzymes. Absence of either FtsW1 or of all three RodA proteins is
112 lethal under standard laboratory conditions. *L. monocytogenes* infections are usually treated
113 with high doses of ß-lactam antibiotics such as ampicillin, which inhibit the transpeptidase
114 activity of PBPs (Swaminathan and Gerner-Smidt, 2007). We demonstrate that the expression

115 of two SEDS proteins, FtsW2 and RodA3, is induced in the presence of ß-lactam antibiotics
116 likely to compensate for the inhibition of PBPs and that a *rodA3* mutant is more sensitive to
117 the ß-lactam antibiotic cefuroxime. Antimicrobials inhibiting the activity of proteins of the
118 SEDS family could therefore potentially improve the treatment of *Listeria* infections in the
119 future.
120

121 **Materials and Methods**

122 **Bacterial strains and growth conditions**

123 All strains and plasmids used in this study are listed in Table S1. Strain and plasmid
124 constructions are described in the supplemental materials and method section and all primers
125 used in this study are listed in Table S2. *E. coli* strains were grown in Luria-Bertani (LB)
126 medium and *L. monocytogenes* strains in brain heart infusion (BHI) medium at 37°C unless
127 otherwise stated. If necessary, antibiotics and supplements were added to the medium at the
128 following concentrations: for *E. coli* cultures, ampicillin (Amp) at 100 µg/ml and kanamycin
129 (Kan) at 30 µg/ml, and for *L. monocytogenes* cultures, chloramphenicol (Cam) at 10 µg/ml,
130 kanamycin (Kan) at 30 µg/ml and Isopropyl β-D-1-thiogalactopyranoside (IPTG) at 1 mM.
131 We used the *L. monocytogenes* strain 10403S and derivatives thereof. However, we refer to
132 *L. monocytogenes* EGD-e gene and locus tag numbers as this was the first fully sequenced *L.*
133 *monocytogenes* strain.
134

135 **Growth curves**

136 Overnight cultures of wildtype *L. monocytogenes* 10403S and the indicated deletion strains
137 were diluted to an OD_{600} of 0.01 or 0.05 in 15 ml BHI medium and the cultures were
138 incubated at 37°C with shaking. Growth was monitored by determining OD_{600} readings at
139 hourly intervals. For growth curves with the IPTG-inducible depletion strains 10403SΔ*ftsW1*
140 i*ftsW* (ANG4314), 10403SΔ*ftsW1* i*ftsW2* (ANG5119) and 10403SΔ*rodA1-3* i*rodA1*

141 (ANG5192), the strains were cultivated overnight in the presence of 1 mM IPTG. The next
142 day, cells were washed once with fresh medium, subsequently diluted 1:50 in 5 ml BHI
143 medium and grown for 8-10 h in the absence of the inducer. The cultures were diluted 1:100
144 into fresh BHI medium and grown until the next morning at 37°C. The depleted cells were
145 then diluted to an OD_{600} of 0.01 and grown in the presence or absence of 1 mM IPTG at
146 37°C. Averages and standard deviations from three independent experiments were plotted.
147
148 **Determination of minimal inhibitory concentration (MIC)**
149 The minimal inhibitory concentration for bacitracin, penicillin and moenomycin and
150 lysozyme was determined using a microbroth dilution assay in 96-well plates. Approximately
151 10^4 *L. monocytogenes* cells were used to inoculate 200 µl BHI containing two-fold dilutions
152 of the different antimicrobials. The starting antibiotic concentrations were: 1 mg/ml for
153 bacitracin A, 1 µg/ml for penicillin G, 0.8 or 1.6 µg/ml for moenomycin, 8 µg/ml cefuroxime
154 and 10 mg/ml for lysozyme. The OD_{600} was determined after incubating the 96-well plates
155 for 24 h at 37°C with shaking at 500 rpm in a plate incubator (Thermostar, BMG Labtech).
156 The MIC value refers to the antibiotic concentration at which bacterial growth was inhibited
157 by >90%.
158
159 **Determination of antibiotic susceptibility using a spot plating assay**
160 Overnight cultures of the indicated *L. monocytogenes* strains were adjusted to an OD_{600} of 1
161 and 5 µl of serial dilutions were spotted on BHI agar plates or BHI agar plates containing 1
162 µg/ml cefuroxime. Plates were photographed after incubation at 37°C for 24 h.
163 **Fluorescence and phase contrast microscopy**
164 For bacterial cell length measurements, 100 µl of mid-log cultures were mixed with 5 µl of
165 100 µg/ml nile red solution to stain the cell membrane. After an incubation of 20 min at

166 37°C, the cells were washed once with 1x PBS and resuspended in 50 µl 1x PBS. 1.5 µl of
167 the different samples were spotted on microscope slides covered with a thin agarose film (1.5
168 % agarose in distilled water), air-dried and covered with a cover slip. Phase contrast and
169 fluorescence images were taken at 100x magnification using the Zeiss Axio Imager.A1
170 microscope coupled to the AxioCam MRm and processed using the Zen 2012 software (blue
171 edition). For the detection of nile red fluorescence signals, the Zeiss filter set 00 was used.
172 For the determination of the cell lengths, 300 cells were measured for each experiment and
173 the median cell length was calculated. Averages and standard deviations of the median cell
174 length of three independent experiments were plotted.
175
176 **Peptidoglycan isolation and analysis**
177 Overnight cultures of *L. monocytogenes* 10403S, 10403SΔ*rodA1*Δ*rodA3* and
178 10403SΔ*rodA1*Δ*rodA3* pIMK3-*rodA1* were used to inoculate 1 L BHI broth (with 1 mM
179 IPTG for the complementation strain 10403SΔ*rodA1*Δ*rodA3* pIMK3-*rodA1*) to a starting
180 OD_{600} of 0.06. The cultures were grown at 37°C until they reached an OD_{600} of 1, at which
181 point the cultures were cooled on ice for 1 h. The bacteria were subsequently collected by
182 centrifugation and peptidoglycan was purified and digested with mutanolysin as described
183 previously (de Jonge et al., 1992, Corrigan et al., 2011). Digested muropeptides were
184 analyzed by high-performance liquid chromatography (HPLC) and recorded at an absorption
185 of 205 nm as described previously (de Jonge et al., 1992). For quantification, the areas of the
186 main muropeptide peaks were integrated using the Agilent Technology ChemStation
187 software. The sum of the peak areas was set to 100% and individual peak areas were
188 determined. Averages and standard deviations from three independent extractions were
189 calculated.
190

191 **β-galactosidase assay**

192 For the determination of the β-galactosidase activity, overnight cultures of strains 10403S
193 pPL3e-$P_{lmo2689}$-*lacZ*, 10403SΔ*rodA1* pPL3e-$P_{lmo2689}$-*lacZ* and 10403SΔ*rodA1*Δ*rodA2* pPL3e-
194 $P_{lmo2689}$-*lacZ* were diluted 1:100 in fresh BHI medium and grown for 6 h at 37°C. Sample
195 collection and preparation were performed as described previously (Gründling et al., 2004).
196 Briefly, OD_{600} readings were determined (for the final β-galactosidase unit calculations) for
197 the different cultures after 6 h of growth and cells from 1 ml culture were pelleted by
198 centrifugation for 10 min at 13,200 x g, resuspended in 100 µl ABT buffer (60 mM K_2HPO_4,
199 40 mM KH_2PO_4, 100 mM NaCl, 0.1% Triton X-100, pH 7.0, filter sterilized), snap frozen in
200 liquid nitrogen and stored at -80°C until use. For the identification of substances inducing the
201 expression of the *lmo2689-lmo2686* operon, an overnight culture of strain 10403S pPL3e-
202 $P_{lmo2689}$-*lacZ* was diluted 1:100 in fresh BHI medium and the culture incubated with shaking
203 at 37°C until an OD_{600} of 0.5-0.6. The culture was divided into several flasks and incubated
204 for two hours at 37°C in the presence or absence of the following substances: 0.5 µg/ml
205 ampicillin, 0.05 µg/ml penicillin, 0.5 µg/ml vancomycin, 4 µg/ml cefuroxime, 0.05 µg/ml
206 moenomycin, 0.5 mg/ml lysozyme, 1% ethanol, 300 µg/ml $MgSO_4$ or 300 µg/ml EDTA.
207 After 2 h, bacterial cultures were harvested and frozen as described above.

208 Samples were thawed and 1:10 dilutions were prepared in ABT buffer. 50 µl of the 1:10
209 diluted samples were mixed with 10 µl of 0.4 mg/ml 4-methyl-umbelliferyl-ß-D-
210 galactopyranoside (MUG) substrate prepared in DMSO and incubated for 60 min at room
211 temperature (RT). A reaction with ABT buffer alone was used as negative control. Following
212 this incubation step, 20 µl of each reaction was diluted into 180 µl of ABT buffer in a black
213 96-well plate and fluorescence values were measured using an HIDEX Sense Microplate
214 Reader at 355 nm excitation and 460 nm emission wavelengths. 0.125-20 µM of the
215 fluorescent 4-methylumbelliferone (MU) standard were used to obtain a standard curve. β-

galactosidase units were calculated as (pmol of substrate hydrolyzed x dilution factor)/(ml culture volume x OD_{600} x minute). The amount of hydrolyzed substrate was determined from the standard curve as (emission reading – y intercept)/slope.

Results

L. monocytogenes 10403S encodes six FtsW/RodA homologs

So far, FtsW and RodA proteins of the human pathogen *L. monocytogenes* have not been studied. FtsW and RodA are members of the SEDS (shape, elongation, division, sporulation) family of proteins and are multispanning membrane proteins with 8-10 transmembrane helices and a large extracellular loop (Fig. 1A). Using BLAST, six proteins with homology to the *B. subtilis* FtsW and RodA proteins could be identified in the genome of *L. monocytogenes* 10403S (Tab. 1). The protein encoded by *lmo0421* has the weakest homology to *B. subtilis* FtsW and RodA (Fig. S1, Tab. 1). *lmo0421* is part of the *sigC* operon, which is comprised of *lmo0422* encoding the PadR-like repressor LstR and *lmo0423* coding for the ECF-type sigma factor SigC (Fig. 1B). The *sigC* operon acts as a lineage II specific heat shock system (Zhang et al., 2005) and is therefore not encoded in all *L. monocytogenes* genomes. Due to the weak homology to FtsW and RodA and its absence in *L. monocytogenes* strains of lineage I and III, Lmo0421 was excluded from further analysis.

The *L. monocytogenes* protein Lmo1071 is the closest homolog to *B. subtilis* FtsW with a sequence identity of 48% (Table 1). Furthermore, *L. monocytogenes lmo1071* and *B. subtilis ftsW* are found in the same chromosomal context. More specifically, *lmo1071* is located between genes *lmo1070*, which encodes a protein with homology to the *B. subtilis* YlaN protein, and *pycA* coding for the pyruvate carboxylase. This analysis suggests that gene *lmo1071* encodes the cell division protein FtsW. However, *L. monocytogenes* encodes a second protein, Lmo2688, that shares a higher degree of homology to the *B. subtilis* FtsW as

241 compared to the *B. subtilis* RodA protein (Table 1). Due to these similarities and additional
242 data presented in this study, we refer to Lmo1071 and Lmo2688 as FtsW1 and FtsW2,
243 respectively.
244 The BLAST search with the *B. subtilis* RodA sequence as a query sequence yielded the *L.*
245 *monocytogenes* protein Lmo2428 as the closest homolog with a sequence identity of 40%
246 (Table 1). In addition to Lmo2428, two additional RodA homologs are present in *L.*
247 *monocytogenes*, namely Lmo2427 and Lmo2687. As presented below, Lmo2427, Lmo2428
248 and Lmo2687 are likely bona-fide RodA homologs and were therefore renamed RodA1,
249 RodA2 and RodA3, respectively. *rodA1* is located adjacent to *rodA2*, but despite their
250 proximity, *rodA1* and *rodA2* are likely not transcribed as part of the same operon (Toledo-
251 Arana et al., 2009). In contrast, *rodA3* and *ftsW2* are part of the four-gene operon *lmo2689-*
252 *lmo2686*. Lmo2689 is similar to a Mg^{2+}-type ATPase, whereas *lmo2686* encodes a protein of
253 unknown function.
254
255 ***lmo1071* encodes FtsW1 and is essential for the survival of *L. monocytogenes***
256 The cell division protein FtsW is essential for growth in the Gram-negative and Gram-
257 positive model organisms *E. coli* and *B. subtilis* (Boyle et al., 1997, Ikeda et al., 1989,
258 Khattar et al., 1994, Kobayashi et al., 2003). Depletion of FtsW in these organisms leads to a
259 block in cell division and formation of elongated cells (Boyle et al., 1997, Gamba et al.,
260 2016). All our attempts to delete the *ftsW1* gene in *L. monocytogenes* 10403S remained
261 unsuccessful, suggesting that FtsW1 is also essential for growth in *Listeria*. Next, strain
262 10403SΔ*ftsW1* i*ftsW1* was constructed, in which the expression of *ftsW1* is controlled by an
263 IPTG-inducible promoter. While no difference in the growth was observed between the
264 wildtype and FtsW1-depletion strain (likely due to leakiness of the inducible promoter) (Fig.
265 2A), cells depleted for FtsW1 were significantly elongated (Fig. 2B-C). Bacteria depleted for

266 FtsW1 had a median cell length of 3.41±0.16 µm, while wildtype and 10403SΔ*ftsW1* i*ftsW1*
267 bacteria grown in the presence of 1 mM IPTG had a median cell length of 1.85±0.16 µm and
268 1.93±0.07 µm, respectively (Fig. 2C). These data indicate that *lmo1071* encodes the cell
269 division specific SEDS protein FtsW.
270
271 ***L. monocytogenes* encodes a second FtsW protein**
272 To our knowledge, all bacteria analyzed to date possess only one FtsW protein that is
273 essential for cell survival. We identified a second potential FtsW protein, Lmo2688, in *L.*
274 *monocytogenes*. In contrast to *ftsW1,* a *L. monocytogenes ftsW2* deletion strain could be
275 constructed and no significant growth or cell morphology phenotypes could be observed for
276 the Δ*ftsW2* deletion strain (data not shown). In a previous study, it was reported that the
277 operon comprised of genes *lmo2689-lmo2686* is only minimally expressed when *L.*
278 *monocytogenes* 10403S is grown in BHI broth (Lobel and Herskovits, 2016). We reasoned
279 that if *ftsW2* does indeed code for a second FtsW protein, it should be possible to delete *ftsW1*
280 in a strain in which *ftsW2* is artificially expressed from an IPTG-inducible promoter. Indeed,
281 strain 10403SΔ*ftsW1* i*ftsW2* could be generated in the presence of IPTG. In contrast, we were
282 unable to generate strain 10403SΔ*ftsW1* when any of the other FtsW/RodA homologs
283 Lmo2427 (RodA1), Lmo2428 (RodA2) or Lmo2687 (RodA3) were expressed from the same
284 IPTG-inducible promoter system. While prolonged depletion of FtsW2 in strain
285 10403SΔ*ftsW1* i*ftsW2* had again no impact on the growth, the cells were significantly
286 elongated in the absence of the inducer compared to wildtype or bacteria grown in the
287 presence of inducer (Fig. 3). These data strongly suggest that *ftsW2* encodes a second FtsW
288 enzyme while the remaining three proteins Lmo2427, Lmo2428 and Lmo2687 likely function
289 as RodA proteins.
290

291 ***L. monocytogenes* encodes three RodA homologs**

292 We were able to assign roles for two of the FtsW/RodA homologs as FtsW-like proteins.
293 However, *L. monocytogenes* encodes three additional homologs, which show a higher
294 similarity to the *B. subtilis* RodA protein as compared to the *B. subtilis* FtsW protein (Tab. 1).
295 As described above, expression of none of the enzymes Lmo2427, Lmo2428 or Lmo2687
296 was able to rescue the growth of an *ftsW1* deletion strain, indicating that these enzymes likely
297 function as RodA proteins in *L. monocytogenes* and hence they were renamed RodA1,
298 RodA2 and RodA3, respectively. All attempts to construct a *rodA1-3* triple mutant failed
299 further corroborating that these proteins function as RodA proteins and at least one of them
300 needs to be present for cell viability. To determine whether the different RodA homologs
301 have distinct functions or whether they are merely duplications, single and double mutant
302 strains were generated. No significant differences with regards to growth and cell length
303 could be observed between the wildtype strain 10403S and single *rodA1*, *rodA2* or *rodA3*
304 deletion strains (Fig. S2). Similar observations were made with the *rodA* double mutant
305 strains 10403SΔ*rodA1*Δ*rodA2* and 10403SΔ*rodA2*Δ*rodA3* (Fig. 4). However, cells lacking
306 RodA1 and RodA3 were shorter (1.3±0.03 µm) compared to wildtype cells (1.9±0.06 µm,
307 Fig. 4B-C), indicating that either RodA1 or RodA3 needs to be present for *L. monocytogenes*
308 to maintain its rod shape. RodA3 is part of the *lmo2689-lmo2686* operon that is only
309 minimally expressed when *L. monocytogenes* is grown in BHI broth (Lobel and Herskovits,
310 2016). The fact that we observe differences in cell morphology between a *rodA1* single and
311 the *rodA1/rodA3* double mutant, suggests that *rodA3* expression might increase upon deletion
312 of *rodA1*. To test this hypothesis, we fused the promoter upstream of *lmo2689* and driving
313 *rodA3* expression to *lacZ* and inserted this fusion into the chromosome of wildtype 10403S,
314 the *rodA1* and the *rodA1/rodA2* deletion strains. The promoter activity was indeed 1.5- to 2-
315 fold increased in the *rodA1* and *rodA1/rodA2* mutant strains as compared to the wildtype, as

316 assessed by the increase in the ß-galactosidase activity (Fig. 4G). This result indicates that
317 expression of the *lmo2689-lmo2686* operon, which encodes FtsW2 and RodA3, is induced in
318 the absence of RodA1, suggesting a coordination of the expression of the different RodA
319 homologs.
320 To confirm that the decrease in cell length of the double mutant strain 10403SΔ*rodA1*Δ*rodA3*
321 depends on the absence of RodA1 and RodA3, complementation strains with IPTG-inducible
322 expression of *rodA1* or *rodA3* were constructed. Expression of RodA1 restored the cell length
323 to 1.84±0.1 µm, which is comparable to the cell length of wildtype cells (1.76±0.15 µm, Fig.
324 4E). On the other hand, expression of RodA3 from the ectopic locus in strain
325 10403SΔ*rodA1*Δ*rodA3* led to the formation of longer cells with an average cell length of
326 2.47±0.01 µm (Fig. 4D-E). These results indicate that induction of RodA3 from the IPTG-
327 inducible promoter likely results in an overproduction of the protein as compared to the
328 expression from the native promoter, highlighting that in particular fine-tuning of RodA3
329 production is essential for cell-length determination in *L. monocytogenes*.
330 The observation that the *rodA1*/*rodA3* double mutant forms shorter cells suggests that RodA2
331 is not sufficient to maintain the cell length of *L. monocytogenes*. There are several possible
332 explanations for this: 1. RodA2 might have a reduced activity as compared to RodA1 or
333 RodA3. 2. RodA2 might have a function that is different from RodA1 and RodA3. 3. The
334 protein levels of RodA2 might be sufficient to maintain cell viability but too low to maintain
335 the rod shape. To determine which of these possibilities might be the case, a strain was
336 constructed which lacks *rodA1* and *rodA3*, but carries pIMK3-*rodA2* to allow for IPTG-
337 inducible expression of *rodA2* in addition to the expression of *rodA2* from its native locus
338 (10403SΔ*rodA1*Δ*rodA3* i*rodA2*). In the absence of the inducer, the cells had a median cell
339 length of 1.2±0.03 µm (data not shown). However, the cell length of strain
340 10403SΔ*rodA1*Δ*rodA3* i*rodA2* increased to 1.71±0.8 µm when the strain was grown in the

341 presence of IPTG (Fig. 4F). Therefore, additional expression of RodA2 can partially
342 complement the cell length phenotype of the *rodA1*/*rodA3* deletion strain, suggesting that
343 RodA2 has a similar function as RodA1 and RodA3, but that it has either a lower activity or
344 is not expressed in sufficient amounts.
345
346 As stated above, several attempts to construct a strain inactivated for all three RodA
347 homologs remained unsuccessful, suggesting that at least one of the proteins RodA1, RodA2
348 or RodA3 needs to be present for the viability of *L. monocytogenes*. The results presented so
349 far indicate that RodA1 is the most important RodA homolog considering that RodA2 alone
350 is not sufficient to maintain the rod shape and that RodA3 is only minimally expressed under
351 standard laboratory conditions (Lobel and Herskovits, 2016). To understand the impact of
352 RodA enzymes on cell growth and cell division in *L. monocytogenes*, a strain was
353 constructed which lacks all three *rodA* genes from its genome, but harbors pIMK3-*rodA1* to
354 enable IPTG-inducible expression of RodA1. Prolonged depletion of RodA1 in strain
355 10403SΔ*rodA1-3* i*rodA1* led to a growth defect that was not seen when the strain was grown
356 in the presence of the inducer (Fig. 5A). However, the depletion was not efficient enough to
357 see a complete growth inhibition, which would be expected for a strain lacking all three
358 RodA homologs. Cells of the *L. monocytogenes* strain 10403SΔ*rodA1-3* i*rodA1* that were
359 grown without IPTG were also significantly shorter with a cell length of 1.18±0.08 µm as
360 compared to cells of the double mutant 10403SΔ*rodA1*Δ*rodA3* or the wildtype strain 10403S
361 (Fig. 5B, D). Interestingly, different cell morphologies could be observed for strain
362 10403SΔ*rodA1-3* i*rodA1* after prolonged RodA1 depletion (Fig. 5C). The placement of the
363 division septum was affected in some cells and daughter cells of different size or cells with
364 two septa were observed (Fig. 5C). These morphological defects could be complemented and
365 the cell length increased to 1.95±0.04 µm upon addition of IPTG and expression of RodA1

366 (Fig. 5D). These data highlight that RodA1 alone is sufficient to maintain the cell shape of *L.*
367 *monocytogenes*.
368
369 **Decreased moenomycin and lysozyme resistance in the absence of RodA homologs**
370 Next, we wondered whether the absence of FtsW or RodA proteins affects the resistance of *L.*
371 *monocytogenes* towards the antibiotics penicillin, bacitracin and moenomycin, which target
372 different steps in the peptidoglycan biosynthesis process. Penicillin binds to the
373 transpeptidase domain of PBPs and inhibits their function, leading to a reduced crosslinking
374 of the peptidoglycan (Nakagawa et al., 1979, Korsak et al., 2010). Bacitracin inhibits the
375 dephosphorylation of the bactoprenol carrier leading to a block in lipid II synthesis (Stone
376 and Strominger, 1971). The phosphoglycolipid antibiotic moenomycin inhibits the
377 glycosyltransferase activity of bifunctional PBPs and thereby prevents the polymerization of
378 the glycan chain (van Heijenoort et al., 1987).
379 No significant differences could be observed in terms of resistance against penicillin,
380 bacitracin or moenomycin for the FtsW1 depletion strain 10403SΔ*ftsW1* i*ftsW1*. This is
381 presumably due to basal level expression of *ftsW1* even in the absence of the inducer (data
382 not shown). Simultaneous deletion of *rodA1* and *rodA3* resulted in a slight decrease in the
383 MIC for penicillin, however, this difference was not significant (Fig. 6A). However, strain
384 10403SΔ*rodA1*Δ*rodA3* was 2-4-fold more sensitive to the antibiotic bacitracin (Fig. 6B). This
385 phenotype could be complemented by expressing either RodA1, RodA2 or RodA3 from an
386 IPTG-inducible promoter (Fig. 6B).
387 As described above, moenomycin inhibits the transglycosylase activity of PBPs leading to a
388 decreased activity of these enzymes. In the absence of RodA1 and RodA3, cells are more
389 susceptible to a reduced activity of PBPs manifesting in a 4-fold reduced resistance to
390 moenomycin (Fig 6C). Induction of RodA1 expression in the 10403SΔ*rodA1*Δ*rodA3* deletion

391 strain resulted in a significantly higher resistance to moenomycin as compared to the
392 wildtype strain 10403S and expression of RodA2 or RodA3, led to partial or complete
393 complementation of the moenomycin sensitivity (Fig. 6C).
394 Moreover, resistance to lysozyme, an enzyme that cleaves the linkage between N-acetyl
395 muramic acid and N-acetylglucosamine residues of the peptidoglycan, was drastically
396 decreased in strain 10403SΔ*rodA1*Δ*rodA3* and could be fully restored by expression of
397 RodA1, RodA2 or RodA3 (Fig. 6D).
398 Lysozyme resistance in *L. monocytogenes* is mainly accomplished by two modifications of
399 the peptidoglycan; deacetylation of N-acetylglucosamine residues by PgdA or O-acetylation
400 of N-acetylmuramic acid residues by OatA (Boneca et al., 2007, Aubry et al., 2011). To
401 determine whether the activity of PgdA is changed in the absence of RodA1 and RodA3,
402 peptidoglycan was purified from the 10403SΔ*rodA1*Δ*rodA3* mutant strain, digested with
403 mutanolysin and the resulting muropeptides analyzed by HPLC. Peptidoglycan samples
404 isolated from the wildtype strain 10403S and the complementation strain
405 10403SΔ*rodA1*Δ*rodA3* i*rodA1*, that had been grown in the presence of IPTG, were analyzed
406 as controls (Fig. 6E). The main muropeptide peaks were assigned as described previously
407 (Rismondo et al., 2015, Burke et al., 2014). Peaks 1 and 2 correspond to the acetylated and
408 deacetylated monomeric muropeptides, respectively, whereas peak 3 and peaks 4-6 are
409 acetylated and deacetylated muropeptide dimers, respectively. Deletion of *rodA1* and *rodA3*
410 led to a reduction of both monomeric muropeptides and therefore to an increase in
411 crosslinked peptidoglycan fragments by approximately 2% as compared to the wildtype strain
412 10403S, in which 65% of the peptidoglycan was cross-linked (Fig. 6F). However, no
413 significant difference with regards to the deacetylated muropeptides could be observed
414 between the wildtype 10403S, the 10403SΔ*rodA1*Δ*rodA3* and the 10403SΔ*rodA1*Δ*rodA3*
415 i*rodA1* complementation strain (Fig. 6F). These results suggest that the lysozyme sensitivity

416 phenotype of strain 10403S*Δ*rodA1*Δ*rodA3* is not caused by changes in the peptidoglycan
417 deacetylation, but rather due to general defects in the peptidoglycan structure.
418
419 **Cell wall-acting antibiotics induce the promoter of *lmo2689***
420 The operon *lmo2689-lmo2686*, that contains the genes encoding FtsW2 and RodA3, is only
421 minimally expressed under standard laboratory conditions (Lobel and Herskovits, 2016).
422 However, a genome-wide transcriptional analysis performed in *L. monocytogenes* strain
423 LO28 has shown that *lmo2687, lmo2688* and *lmo2689* are part of the CesR regulon (Nielsen
424 et al., 2012). The cephalosporin sensitivity response regulator CesR is part of the CesRK two-
425 component system that regulates the transcription of several cell envelope-related genes in
426 response to changes in cell wall integrity, such as caused by the presence of cell wall-acting
427 antibiotics or alcohols such as ethanol (Gottschalk et al., 2008, Kallipolitis et al., 2003,
428 Nielsen et al., 2012). Therefore, we next used the *lmo2689* promoter-*lacZ* fusion described
429 above, to assess if expression of the *lmo2689-lmo2686* operon is induced in the presence of
430 antibiotics that target different processes of the PG biosynthesis or ethanol. Indeed, increased
431 β-galactosidase activity could be measured for cells that had been grown in the presence of
432 sub-inhibitory concentrations of the β-lactam antibiotics ampicillin, penicillin and cefuroxime
433 and the phosphoglycolipid moenomycin (Fig. 7A). In contrast, no increase in β-galactosidase
434 activity could be detected upon addition of vancomycin, lysozyme or ethanol as compared to
435 untreated control cells (Fig. 7A). We also tested whether the presence of $MgSO_4$ or EDTA
436 has an impact on the *lmo2689* promoter activity since *lmo2689* encodes a putative Mg^{2+}-type
437 ATPase. However, the β-galactosidase activity of cells grown in the presence of $MgSO_4$ or
438 EDTA was comparable to the β-galactosidase activity seen for untreated cells (Fig. 7A).
439 These results indicate that the expression of *ftsW2* and *rodA3*, that are part of the *lmo2689-*
440 *lmo2686* operon, are induced in the presence of various cell wall-acting antibiotics,

441 suggesting that FtsW2 and RodA3 might be important for the intrinsic resistance of *L.*
442 *monocytogenes* against these antibiotics. However, no significant differences in MICs for
443 penicillin and moenomycin could be observed between wildtype 10403S, the *ftsW2* or *rodA3*
444 single mutant strains or the *ftsW2/rodA3* double mutant (Fig. S3). However, there was a slight
445 reduction in the resistance of the *rodA3* single mutant against cefuroxime as compared to the
446 wildtype (Fig. S3). To further assess whether there is a difference in the cefuroxime
447 resistance between the *L. monocytogenes* wildtype strain 10403S and the *rodA1*, *rodA2* and
448 *rodA3* single mutant strains, dilutions of overnight cultures were spotted on BHI agar plates
449 with or without 1 µg/ml cefuroxime. Deletion of *rodA1* or *rodA2* results in a slightly reduced
450 ability of these strains to grow on BHI plates supplemented with 1 µg/ml cefuroxime as
451 compared to the wildtype 10403S strain (Fig. 7B). However, deletion of *rodA3* leads to a
452 stronger reduction of growth on BHI plates containing 1 µg/ml cefuroxime as compared to
453 the *rodA1* and *rodA2* single mutants (Fig. 7B). Our results therefore suggest that *L.*
454 *monocytogenes* induces the expression of *rodA3* and *ftsW2* in the presence of β-lactam
455 antibiotics and moenomycin to compensate for the inhibition of the glycosyltransferase and
456 transpeptidase activity of PBPs and that in particular the RodA homolog RodA3 has an
457 important function for the intrinsic antibiotic resistance of *L. monocytogenes*.
458

459 **Discussion**

460 Bacterial cell elongation and cell division need to be tightly regulated to maintain the cell
461 shape. This is accomplished by two multiprotein complexes, the rod complex and the
462 divisome, which are coordinated by the actin homolog MreB and the tubulin homolog FtsZ,
463 respectively (Ricard and Hirota, 1973, Nanninga, 1991, Carballido-Lopez and Formstone,
464 2007, Typas et al., 2012, Jones et al., 2001, Bi and Lutkenhaus, 1991). The SEDS protein
465 FtsW is part of the divisome and essential for growth as shown for many bacteria including

466 *E. coli, B. subtilis* and *S. aureus* (Boyle et al., 1997, Ikeda et al., 1989, Khattar et al., 1994,
467 Kobayashi et al., 2003, Reichmann et al., 2019). Our experiments suggested that FtsW1 is
468 also essential in *L. monocytogenes*, however, a second FtsW protein, FtsW2, can compensate
469 for the loss of FtsW1 if it is expressed from an inducible promoter. FtsW2 is encoded in the
470 *lmo2689-lmo2686* operon that appears to be only minimally expressed when *L.*
471 *monocytogenes* 10403S is grown under standard laboratory conditions (Lobel and Herskovits,
472 2016). The expression of the *lmo2689-lmo2686* operon is regulated by the two-component
473 system CesRK that is activated by cell envelope stress (Kallipolitis et al., 2003, Gottschalk et
474 al., 2008, Nielsen et al., 2012). Using an *L. monocytogenes* strain carrying a $P_{lmo2689}$-*lacZ*
475 promoter fusion, we could detect increased β-galactosidase activity after incubation with sub-
476 inhibitory concentrations of different β-lactam antibiotics including penicillin, cefuroxime,
477 and moenomycin. However, the expression of the *lmo2689-lmo2686* operon was not induced
478 by other cell wall-targeting antibiotics such as vancomycin or the hydrolase lysozyme. This
479 suggests that inhibition of the glycosyltransferase or transpeptidase activity of PBPs leads to
480 activation of the *lmo2689-lmo2686* operon, and hence, to the expression of *ftsW2* as well as
481 *rodA3*.
482 The rod-shape determining protein RodA is part of the elongation machinery. The data
483 presented in this study suggest that *L. monocytogenes* encodes not one but three RodA
484 proteins and depletion of the three RodA enzymes leads to a decreased cell length (Fig. 5).
485 Simultaneous deletion of *rodA1* and *rodA3* already results in the formation of shorter cells,
486 whereas cells of strains deleted for *rodA1/rodA2* or *rodA2/rodA3* have a cell length that is
487 comparable to the wildtype strain 10403S. Taking into consideration that *rodA3* is only
488 minimally expressed under standard laboratory growth conditions in *L. monocytogenes*
489 10403S (Lobel and Herskovits, 2016), the results presented in this study suggest that *rodA3*
490 expression gets induced upon inactivation of RodA1, since we observed morphological

491 differences between the *rodA1* single and the *rodA1/3* double mutant strains. Indeed, β-
492 galactosidase assays confirmed that deletion of *rodA1* or *rodA1/2* increases the activity of the
493 promoter from which *rodA3* is expressed. The data presented in this study also indicate that
494 RodA1 is the "main" RodA enzyme in *L. monocytogenes* as no significant phenotypic
495 changes with regards to growth and cell division could be observed as long as RodA1 was
496 present. On the other hand, RodA2 was only able to compensate for the loss of RodA1 and
497 RodA3, when overproduced from an inducible promoter. This suggests that either RodA2 has
498 a reduced activity compared to RodA1 or RodA3, which can be overcome by overproducing
499 the enzyme, or the expression levels of RodA2 are too low to maintain the cell shape.
500 Interestingly, cells of strain 10403SΔ*rodA1*Δ*rodA3* in which *rodA3* is overexpressed from an
501 ectopic locus have an increased cell length as compared to the wildtype. An explanation for
502 this could be that elevated levels of RodA3 lead to the depletion of proteins needed at the cell
503 division site, resulting in an extended synthesis of PG on the lateral wall. Another possibility
504 could be that RodA3 directly inhibits FtsW1 or displaces FtsW1 at the cell division site,
505 leading to a block in cell division and therefore resulting in the formation of elongated cells.
506 Further experiments are needed to distinguish between these possibilities.
507 Recent studies have shown that SEDS proteins acts as glycosyltransferases (Meeske et al.,
508 2016, Emami et al., 2017). The glycosyltransferase activity of PBPs and MGT can be
509 inhibited by moenomycin, whereas RodA/FtsW enzymes are not affected by moenomycin
510 and are therefore important for moenomycin resistance (Tamura et al., 1980, Emami et al.,
511 2017). In good agreement with this, deletion of the genes encoding two of the three RodA
512 enzymes, RodA1 and RodA3, resulted in an increased moenomycin sensitivity of *L.*
513 *monocytogenes* (Fig. 7B).
514 In *B. subtilis*, RodA is in a complex with the class B PBP, PBP 2A (also named PBPH), and
515 these two proteins act together to polymerize and crosslink the glycan strands (Wei et al.,

516 2003, Henriques et al., 1998). Similarly, FtsW and PBP 2B form a subcomplex as part of the
517 divisome (Daniel et al., 1996, Gamba et al., 2009). Recently it was shown that RodA-PBP3
518 and FtsW-PBP1 act as cognate pairs in the coccoid bacterium *S. aureus* (Reichmann et al.,
519 2019). Depletion of all three RodA enzymes in *L. monocytogenes*, RodA1, RodA2 and
520 RodA3, leads to a drastic reduction in cell length (Fig. 5). A similar phenotype was observed
521 for a *L. monocytogenes* strain depleted for the essential class B PBP, PBP B1 (Rismondo et
522 al., 2015). In contrast, the absence of either FtsW1 (Fig.2) or the class B PBP, PBP B2, in *L.*
523 *monocytogenes* results in the formation of elongated cells (Rismondo et al., 2015). These
524 observations suggest that RodA and FtsW might work in a complex with the cognate PBPs
525 PBP B1 and PBP B2 during cell elongation and cell division, respectively. Further studies are
526 necessary to confirm this hypothesis.
527 It is also interesting to note that *L. monocytogenes* does not only encode multiple FtsW/RodA
528 enzymes, but also encodes two copies of the lipid II flippase MurJ, MurJ1 and MurJ2.
529 RNAseq data suggest that *murJ1* and *murJ2* are both expressed in *L. monocytogenes* 10403S
530 when grown in BHI broth (Lobel and Herskovits, 2016). *murJ1* and *murJ2* might therefore
531 solely be gene duplications, however, MurJ1 and MurJ2 might have specific roles in different
532 growth conditions, which needs to be assessed in future studies.
533 Taken together, *L. monocytogenes* has a repertoire of two lipid II flippases, several PBPs and
534 multiple members of the SEDS family of proteins to produce its rigid cell wall. The
535 expression and the activity of these enzymes need to be tightly regulated in *L. monocytogenes*
536 to maintain its cell shape. Our results suggest that *L. monocytogenes* adapts the expression of
537 two FtsW/RodA enzymes, FtsW2 and RodA3, to environmental stresses such as the presence
538 of β-lactam antibiotics, thereby preventing defects in the peptidoglycan synthesis and
539 subsequent cell lysis.
540

Acknowledgements

This work was funded by the Wellcome Trust grants 100289/Z/12/Z and 210671/Z/18/Z to AG and the German research foundation (DFG) grant RI 2920/1-1 to JR.

546 **References**
547

548 AUBRY, C., GOULARD, C., NAHORI, M. A., CAYET, N., DECALF, J., SACHSE, M.,
549 BONECA, I. G., COSSART, P. & DUSSURGET, O. 2011. OatA, a peptidoglycan O-
550 acetyltransferase involved in *Listeria monocytogenes* immune escape, is critical for
551 virulence. *J Infect Dis,* 204**,** 731-40.
552 BI, E. F. & LUTKENHAUS, J. 1991. FtsZ ring structure associated with division in
553 *Escherichia coli*. *Nature,* 354**,** 161-4.
554 BLUMBERG, P. M. & STROMINGER, J. L. 1974. Interaction of penicillin with the
555 bacterial cell: penicillin-binding proteins and penicillin-sensitive enzymes. *Bacteriol*
556 *Rev,* 38**,** 291-335.
557 BONECA, I. G., DUSSURGET, O., CABANES, D., NAHORI, M. A., SOUSA, S., LECUIT,
558 M., PSYLINAKIS, E., BOURIOTIS, V., HUGOT, J. P., GIOVANNINI, M.,
559 COYLE, A., BERTIN, J., NAMANE, A., ROUSSELLE, J. C., CAYET, N.,
560 PREVOST, M. C., BALLOY, V., CHIGNARD, M., PHILPOTT, D. J., COSSART,
561 P. & GIRARDIN, S. E. 2007. A critical role for peptidoglycan N-deacetylation in
562 *Listeria* evasion from the host innate immune system. *Proc Natl Acad Sci U S A,* 104**,**
563 997-1002.
564 BOYLE, D. S., KHATTAR, M. M., ADDINALL, S. G., LUTKENHAUS, J. & DONACHIE,
565 W. D. 1997. *ftsW* is an essential cell-division gene in *Escherichia coli*. *Mol Microbiol,*
566 24**,** 1263-73.
567 BURKE, T. P., LOUKITCHEVA, A., ZEMANSKY, J., WHEELER, R., BONECA, I. G. &
568 PORTNOY, D. A. 2014. *Listeria monocytogenes* is resistant to lysozyme through the
569 regulation, not the acquisition, of cell wall-modifying enzymes. *J Bacteriol,* 196**,**
570 3756-67.
571 CARBALLIDO-LOPEZ, R. & FORMSTONE, A. 2007. Shape determination in *Bacillus*
572 *subtilis*. *Curr Opin Microbiol,* 10**,** 611-6.
573 CHO, H., WIVAGG, C. N., KAPOOR, M., BARRY, Z., ROHS, P. D. A., SUH, H.,
574 MARTO, J. A., GARNER, E. C. & BERNHARDT, T. G. 2016. Bacterial cell wall
575 biogenesis is mediated by SEDS and PBP polymerase families functioning semi-
576 autonomously. *Nature Microbiology,* 1**,** 16172.
577 CORRIGAN, R. M., ABBOTT, J. C., BURHENNE, H., KAEVER, V. & GRÜNDLING, A.
578 2011. c-di-AMP is a new second messenger in *Staphylococcus aureus* with a role in
579 controlling cell size and envelope stress. *PLoS Pathog,* 7**,** e1002217.
580 DANIEL, R. A., WILLIAMS, A. M. & ERRINGTON, J. 1996. A complex four-gene operon
581 containing essential cell division gene *pbpB* in *Bacillus subtilis*. *J Bacteriol,* 178**,**
582 2343-50.
583 DE JONGE, B. L., CHANG, Y. S., GAGE, D. & TOMASZ, A. 1992. Peptidoglycan
584 composition of a highly methicillin-resistant *Staphylococcus aureus* strain. The role
585 of penicillin binding protein 2A. *J Biol Chem,* 267**,** 11248-54.
586 EMAMI, K., GUYET, A., KAWAI, Y., DEVI, J., WU, L. J., ALLENBY, N., DANIEL, R.
587 A. & ERRINGTON, J. 2017. RodA as the missing glycosyltransferase in *Bacillus*
588 *subtilis* and antibiotic discovery for the peptidoglycan polymerase pathway. *Nat*
589 *Microbiol,* 2**,** 16253.
590 FRAIPONT, C., ALEXEEVA, S., WOLF, B., VAN DER PLOEG, R., SCHLOESSER, M.,
591 DEN BLAAUWEN, T. & NGUYEN-DISTECHE, M. 2011. The integral membrane
592 FtsW protein and peptidoglycan synthase PBP3 form a subcomplex in *Escherichia*
593 *coli*. *Microbiology,* 157**,** 251-9.
594 GAMBA, P., HAMOEN, L. W. & DANIEL, R. A. 2016. Cooperative Recruitment of FtsW
595 to the Division Site of *Bacillus subtilis*. *Front Microbiol,* 7**,** 1808.

596 GAMBA, P., VEENING, J. W., SAUNDERS, N. J., HAMOEN, L. W. & DANIEL, R. A.
597 2009. Two-step assembly dynamics of the *Bacillus subtilis* divisome. *J Bacteriol,*
598 191**,** 4186-94.
599 GHUYSEN, J. M. & STROMINGER, J. L. 1963. Structure of the Cell Wall of
600 *Staphylococcus aureus*, Strain Copenhagen. Ii. Separation and Structure of
601 Disaccharides. *Biochemistry,* 2**,** 1119-25.
602 GOFFIN, C. & GHUYSEN, J. M. 1998. Multimodular penicillin-binding proteins: an
603 enigmatic family of orthologs and paralogs. *Microbiol Mol Biol Rev,* 62**,** 1079-93.
604 GOTTSCHALK, S., BYGEBJERG-HOVE, I., BONDE, M., NIELSEN, P. K., NGUYEN, T.
605 H., GRAVESEN, A. & KALLIPOLITIS, B. H. 2008. The two-component system
606 CesRK controls the transcriptional induction of cell envelope-related genes in *Listeria*
607 *monocytogenes* in response to cell wall-acting antibiotics. *J Bacteriol,* 190**,** 4772-6.
608 GRÜNDLING, A., BURRACK, L. S., BOUWER, H. G. & HIGGINS, D. E. 2004. *Listeria*
609 *monocytogenes* regulates flagellar motility gene expression through MogR, a
610 transcriptional repressor required for virulence. *Proc Natl Acad Sci U S A,* 101**,**
611 12318-23.
612 HARA, H. & SUZUKI, H. 1984. A novel glycan polymerase that synthesizes uncross-linked
613 peptidoglycan in *Escherichia coli*. *FEBS Lett,* 168**,** 155-60.
614 HENRIQUES, A. O., DE LENCASTRE, H. & PIGGOT, P. J. 1992. A *Bacillus subtilis*
615 morphogene cluster that includes *spoVE* is homologous to the *mra* region of
616 *Escherichia coli*. *Biochimie,* 74**,** 735-48.
617 HENRIQUES, A. O., GLASER, P., PIGGOT, P. J. & MORAN, C. P., JR. 1998. Control of
618 cell shape and elongation by the *rodA* gene in *Bacillus subtilis*. *Mol Microbiol,* 28**,**
619 235-47.
620 HÖLTJE, J. V. 1998. Growth of the stress-bearing and shape-maintaining murein sacculus of
621 *Escherichia coli*. *Microbiol Mol Biol Rev,* 62**,** 181-203.
622 IKEDA, M., SATO, T., WACHI, M., JUNG, H. K., ISHINO, F., KOBAYASHI, Y. &
623 MATSUHASHI, M. 1989. Structural similarity among *Escherichia coli* FtsW and
624 RodA proteins and *Bacillus subtilis* SpoVE protein, which function in cell division,
625 cell elongation, and spore formation, respectively. *J Bacteriol,* 171**,** 6375-8.
626 JONES, L. J., CARBALLIDO-LOPEZ, R. & ERRINGTON, J. 2001. Control of cell shape in
627 bacteria: helical, actin-like filaments in *Bacillus subtilis*. *Cell,* 104**,** 913-22.
628 KALLIPOLITIS, B. H., INGMER, H., GAHAN, C. G., HILL, C. & SOGAARD-
629 ANDERSEN, L. 2003. CesRK, a two-component signal transduction system in
630 *Listeria monocytogenes*, responds to the presence of cell wall-acting antibiotics and
631 affects beta-lactam resistance. *Antimicrob Agents Chemother,* 47**,** 3421-9.
632 KARINOU, E., SCHUSTER, C. F., PAZOS, M., VOLLMER, W. & GRUNDLING, A.
633 2018. Inactivation of the monofunctional peptidoglycan glycosyltransferase SgtB
634 allows *Staphylococcus aureus* to survive in the absence of lipoteichoic acid. *J*
635 *Bacteriol*.
636 KHATTAR, M. M., BEGG, K. J. & DONACHIE, W. D. 1994. Identification of FtsW and
637 characterization of a new *ftsW* division mutant of *Escherichia coli*. *J Bacteriol,* 176**,**
638 7140-7.
639 KOBAYASHI, K., EHRLICH, S. D., ALBERTINI, A., AMATI, G., ANDERSEN, K. K.,
640 ARNAUD, M., ASAI, K., ASHIKAGA, S., AYMERICH, S., BESSIERES, P.,
641 BOLAND, F., BRIGNELL, S. C., BRON, S., BUNAI, K., CHAPUIS, J.,
642 CHRISTIANSEN, L. C., DANCHIN, A., DEBARBOUILLE, M., DERVYN, E.,
643 DEUERLING, E., DEVINE, K., DEVINE, S. K., DREESEN, O., ERRINGTON, J.,
644 FILLINGER, S., FOSTER, S. J., FUJITA, Y., GALIZZI, A., GARDAN, R.,
645 ESCHEVINS, C., FUKUSHIMA, T., HAGA, K., HARWOOD, C. R., HECKER, M.,

646 HOSOYA, D., HULLO, M. F., KAKESHITA, H., KARAMATA, D., KASAHARA,
647 Y., KAWAMURA, F., KOGA, K., KOSKI, P., KUWANA, R., IMAMURA, D.,
648 ISHIMARU, M., ISHIKAWA, S., ISHIO, I., LE COQ, D., MASSON, A., MAUEL,
649 C., MEIMA, R., MELLADO, R. P., MOIR, A., MORIYA, S., NAGAKAWA, E.,
650 NANAMIYA, H., NAKAI, S., NYGAARD, P., OGURA, M., OHANAN, T.,
651 O'REILLY, M., O'ROURKE, M., PRAGAI, Z., POOLEY, H. M., RAPOPORT, G.,
652 RAWLINS, J. P., RIVAS, L. A., RIVOLTA, C., SADAIE, A., SADAIE, Y.,
653 SARVAS, M., SATO, T., SAXILD, H. H., SCANLAN, E., SCHUMANN, W.,
654 SEEGERS, J. F., SEKIGUCHI, J., SEKOWSKA, A., SEROR, S. J., SIMON, M.,
655 STRAGIER, P., STUDER, R., TAKAMATSU, H., TANAKA, T., TAKEUCHI, M.,
656 THOMAIDES, H. B., VAGNER, V., VAN DIJL, J. M., WATABE, K., WIPAT, A.,
657 YAMAMOTO, H., YAMAMOTO, M., YAMAMOTO, Y., YAMANE, K., YATA,
658 K., YOSHIDA, K., YOSHIKAWA, H., ZUBER, U. & OGASAWARA, N. 2003.
659 Essential *Bacillus subtilis* genes. *Proc Natl Acad Sci U S A,* 100**,** 4678-83.
660 KORSAK, D., MARKIEWICZ, Z., GUTKIND, G. O. & AYALA, J. A. 2010. Identification
661 of the full set of *Listeria monocytogenes* penicillin-binding proteins and
662 characterization of PBPD2 (Lmo2812). *BMC Microbiol,* 10**,** 239.
663 LECLERCQ, S., DEROUAUX, A., OLATUNJI, S., FRAIPONT, C., EGAN, A. J.,
664 VOLLMER, W., BREUKINK, E. & TERRAK, M. 2017. Interplay between
665 Penicillin-binding proteins and SEDS proteins promotes bacterial cell wall synthesis.
666 *Sci Rep,* 7**,** 43306.
667 LIU, X., GALLAY, C., KJOS, M., DOMENECH, A., SLAGER, J., VAN KESSEL, S. P.,
668 KNOOPS, K., SORG, R. A., ZHANG, J. R. & VEENING, J. W. 2017. High-
669 throughput CRISPRi phenotyping identifies new essential genes in *Streptococcus*
670 *pneumoniae*. *Mol Syst Biol,* 13**,** 931.
671 LOBEL, L. & HERSKOVITS, A. A. 2016. Systems Level Analyses Reveal Multiple
672 Regulatory Activities of CodY Controlling Metabolism, Motility and Virulence in
673 *Listeria monocytogenes*. *PLoS Genet,* 12**,** e1005870.
674 MCPHERSON, D. C. & POPHAM, D. L. 2003. Peptidoglycan synthesis in the absence of
675 class A penicillin-binding proteins in *Bacillus subtilis*. *J Bacteriol,* 185**,** 1423-31.
676 MEESKE, A. J., RILEY, E. P., ROBINS, W. P., UEHARA, T., MEKALANOS, J. J.,
677 KAHNE, D., WALKER, S., KRUSE, A. C., BERNHARDT, T. G. & RUDNER, D.
678 Z. 2016. SEDS proteins are a widespread family of bacterial cell wall polymerases.
679 *Nature,* 537**,** 634-638.
680 MEESKE, A. J., SHAM, L. T., KIMSEY, H., KOO, B. M., GROSS, C. A., BERNHARDT,
681 T. G. & RUDNER, D. Z. 2015. MurJ and a novel lipid II flippase are required for cell
682 wall biogenesis in *Bacillus subtilis*. *Proc Natl Acad Sci U S A,* 112**,** 6437-42.
683 NAKAGAWA, J., TAMAKI, S. & MATSUHASHI, M. 1979. Purified penicillin binding
684 proteins 1Bs from *Escherichia coli* membrane showing activities of both
685 peptidoglycan polymerase and peptidoglycan crosslinking enzyme. *Agric. Biol.*
686 *Chem.,* 43**,** 1379-1380.
687 NANNINGA, N. 1991. Cell division and peptidoglycan assembly in *Escherichia coli*. *Mol*
688 *Microbiol,* 5**,** 791-5.
689 NIELSEN, P. K., ANDERSEN, A. Z., MOLS, M., VAN DER VEEN, S., ABEE, T. &
690 KALLIPOLITIS, B. H. 2012. Genome-wide transcriptional profiling of the cell
691 envelope stress response and the role of LisRK and CesRK in *Listeria*
692 *monocytogenes*. *Microbiology,* 158**,** 963-74.
693 PARK, W. & MATSUHASHI, M. 1984. *Staphylococcus aureus* and *Micrococcus luteus*
694 peptidoglycan transglycosylases that are not penicillin-binding proteins. *J Bacteriol,*
695 157**,** 538-44.

696 PARK, W., SETO, H., HAKENBECK, R. & MATSUHASHI, M. 1985. Major peptidoglycan
697 transglycosylase activity in *Streptococcus pneumoniae* that is not a penicillin-binding
698 protein. *FEMS Microbiology Letters,* 27**,** 45-48.
699 PINHO, M. G., KJOS, M. & VEENING, J. W. 2013. How to get (a)round: mechanisms
700 controlling growth and division of coccoid bacteria. *Nat Rev Microbiol,* 11**,** 601-14.
701 REICHMANN, N. T., TAVARES, A. C., SARAIVA, B. M., JOUSSELIN, A., REED, P.,
702 PEREIRA, A. R., MONTEIRO, J. M., VANNIEUWENHZE, M. S., FERNANDES,
703 F. & PINHO, M. G. 2019. SEDS-bPBP pairs direct lateral and septal peptidoglycan
704 synthesis in *Staphylococcus aureus*. *bioRxiv***,** 552034.
705 RICARD, M. & HIROTA, Y. 1973. Process of cellular division in *Escherichia coli*:
706 physiological study on thermosensitive mutants defective in cell division. *J Bacteriol,*
707 116**,** 314-22.
708 RISMONDO, J., MOLLER, L., ALDRIDGE, C., GRAY, J., VOLLMER, W. &
709 HALBEDEL, S. 2015. Discrete and overlapping functions of peptidoglycan synthases
710 in growth, cell division and virulence of *Listeria monocytogenes*. *Mol Microbiol,* 95**,**
711 332-51.
712 ROGERS, H. J., PERKINS, H. R. & WARD, J. B. 1980. Microbial Cell Walls and
713 Membranes. *Chapman and Hall New York, N.Y.,* 10**,** 33-33.
714 RUIZ, N. 2008. Bioinformatics identification of MurJ (MviN) as the peptidoglycan lipid II
715 flippase in *Escherichia coli*. *Proc Natl Acad Sci U S A,* 105**,** 15553-7.
716 SAUVAGE, E., KERFF, F., TERRAK, M., AYALA, J. A. & CHARLIER, P. 2008. The
717 penicillin-binding proteins: structure and role in peptidoglycan biosynthesis. *FEMS*
718 *Microbiol Rev,* 32**,** 234-58.
719 SCHEFFERS, D. J. & PINHO, M. G. 2005. Bacterial cell wall synthesis: new insights from
720 localization studies. *Microbiol Mol Biol Rev,* 69**,** 585-607.
721 SHAM, L. T., BUTLER, E. K., LEBAR, M. D., KAHNE, D., BERNHARDT, T. G. & RUIZ,
722 N. 2014. Bacterial cell wall. MurJ is the flippase of lipid-linked precursors for
723 peptidoglycan biogenesis. *Science,* 345**,** 220-2.
724 SIEVERS, F., WILM, A., DINEEN, D., GIBSON, T. J., KARPLUS, K., LI, W., LOPEZ, R.,
725 MCWILLIAM, H., REMMERT, M., SODING, J., THOMPSON, J. D. & HIGGINS,
726 D. G. 2011. Fast, scalable generation of high-quality protein multiple sequence
727 alignments using Clustal Omega. *Mol Syst Biol,* 7**,** 539.
728 SONNHAMMER, E. L., VON HEIJNE, G. & KROGH, A. 1998. A hidden Markov model
729 for predicting transmembrane helices in protein sequences. *Proc Int Conf Intell Syst*
730 *Mol Biol,* 6**,** 175-82.
731 STONE, K. J. & STROMINGER, J. L. 1971. Mechanism of action of bacitracin:
732 complexation with metal ion and C 55 -isoprenyl pyrophosphate. *Proc Natl Acad Sci*
733 *U S A,* 68**,** 3223-7.
734 SWAMINATHAN, B. & GERNER-SMIDT, P. 2007. The epidemiology of human listeriosis.
735 *Microbes Infect,* 9**,** 1236-43.
736 TAGUCHI, A., WELSH, M. A., MARMONT, L. S., LEE, W., SJODT, M., KRUSE, A. C.,
737 KAHNE, D., BERNHARDT, T. G. & WALKER, S. 2019. FtsW is a peptidoglycan
738 polymerase that is functional only in complex with its cognate penicillin-binding
739 protein. *Nat Microbiol*.
740 TAMURA, T., SUZUKI, H., NISHIMURA, Y., MIZOGUCHI, J. & HIROTA, Y. 1980. On
741 the process of cellular division in *Escherichia coli*: isolation and characterization of
742 penicillin-binding proteins 1a, 1b, and 3. *Proc Natl Acad Sci U S A,* 77**,** 4499-503.
743 TOLEDO-ARANA, A., DUSSURGET, O., NIKITAS, G., SESTO, N., GUET-REVILLET,
744 H., BALESTRINO, D., LOH, E., GRIPENLAND, J., TIENSUU, T.,
745 VAITKEVICIUS, K., BARTHELEMY, M., VERGASSOLA, M., NAHORI, M. A.,

SOUBIGOU, G., REGNAULT, B., COPPEE, J. Y., LECUIT, M., JOHANSSON, J. & COSSART, P. 2009. The *Listeria* transcriptional landscape from saprophytism to virulence. *Nature,* 459**,** 950-6.

TYPAS, A., BANZHAF, M., GROSS, C. A. & VOLLMER, W. 2012. From the regulation of peptidoglycan synthesis to bacterial growth and morphology. *Nat Rev Microbiol,* 10**,** 123-36.

VAN HEIJENOORT, J. 2001. Formation of the glycan chains in the synthesis of bacterial peptidoglycan. *Glycobiology,* 11**,** 25R-36R.

VAN HEIJENOORT, Y., LEDUC, M., SINGER, H. & VAN HEIJENOORT, J. 1987. Effects of moenomycin on *Escherichia coli*. *J Gen Microbiol,* 133**,** 667-74.

VOLLMER, W., BLANOT, D. & DE PEDRO, M. A. 2008. Peptidoglycan structure and architecture. *FEMS Microbiol Rev,* 32**,** 149-67.

WANG, Q. M., PEERY, R. B., JOHNSON, R. B., ALBORN, W. E., YEH, W. K. & SKATRUD, P. L. 2001. Identification and characterization of a monofunctional glycosyltransferase from *Staphylococcus aureus*. *J Bacteriol,* 183**,** 4779-85.

WEI, Y., HAVASY, T., MCPHERSON, D. C. & POPHAM, D. L. 2003. Rod shape determination by the *Bacillus subtilis* class B penicillin-binding proteins encoded by *pbpA* and *pbpH*. *J Bacteriol,* 185**,** 4717-26.

WEIDEL, W. & PELZER, H. 1964. Bagshaped Macromolecules--a New Outlook on Bacterial Cell Walls. *Adv Enzymol Relat Areas Mol Biol,* 26**,** 193-232.

ZHANG, C., NIETFELDT, J., ZHANG, M. & BENSON, A. K. 2005. Functional consequences of genome evolution in *Listeria monocytogenes*: the *lmo0423* and *lmo0422* genes encode sigmaC and LstR, a lineage II-specific heat shock system. *J Bacteriol,* 187**,** 7243-53.

Table 1: Sequence homology between *B. subtilis* and *L. monocytogenes* FtsW/RodA proteins as determined by BLAST.

***L. monocytogenes* proteins**	***B. subtilis* FtsW (403 aa)***	***B. subtilis* RodA (393 aa)***
Lmo0421	46/128 aa (36%)	77/350 aa (22%)
(416 aa)	7e-14	4e-09
FtsW1 (Lmo1071)	195/403 aa (48%)	100/333 aa (30%)
(402 aa)	1e-122	7e-35
RodA1 (Lmo2427)	124/403 aa (31%)	132/360 aa (37%)
(391 aa)	9e-29	1e-57
RodA2 (Lmo2428)	112/374 aa (30%)	159/402 aa (40%)
(389 aa)	1e-33	1e-66
RodA3 (Lmo2687)	95/324 aa (29%)	110/356 aa (31%)
(369 aa)	3e-25	3e-44
FtsW2 (Lmo2688)	147/342 aa (43%)	95/300 aa (32%)
(376 aa)	5e-67	6e-22

* *L. monocytogenes* proteins and their amino acid sizes (aa) are shown in bold in the left column and *B. subtilis* FtsW and RodA proteins used for the homology search are denoted in the top row. The number of amino acids, which were found to be identical between the respective *L. monocytogenes* and *B. subtilis* FtsW/RodA protein are denoted (left number) along with the amino acids that was utilized by the BLAST algorithm for this comparison (right number). The % identity is given in brackets and the corresponding e-values are indicated below.

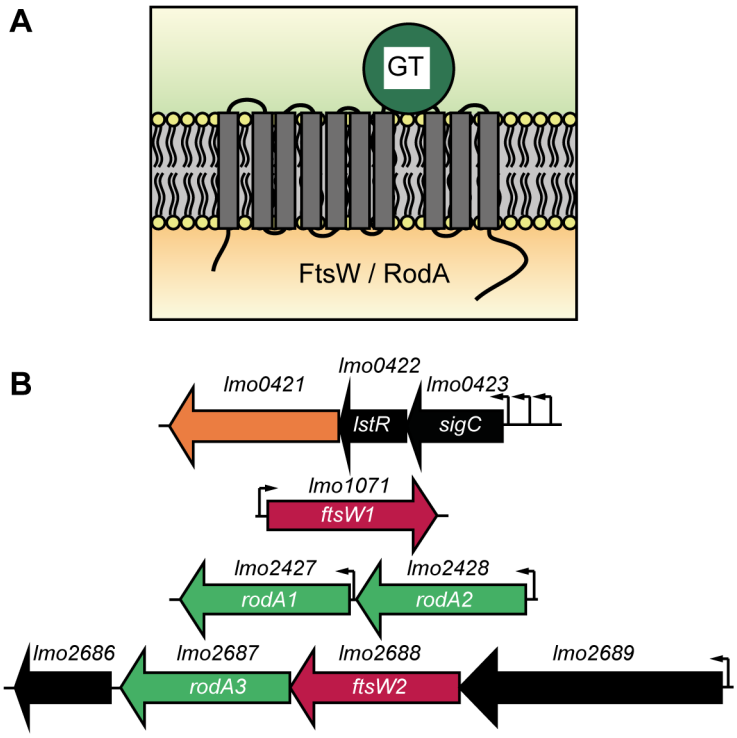

Figure 1: Topology of FtsW and RodA enzymes and their genomic arrangement in *L. monocytogenes.* (A) Topology models for FtsW and RodA enzymes of *L. monocytogenes* as predicted using the TMHMM v. 2.0 server (Sonnhammer et al., 1998). (B) Genomic organization of *ftsW/rodA* genes in *L. monocytogenes.* Arrowheads indicate the gene orientation. Small black arrows indicate promoters based on the operon structures described in Toledo-Arana *et al*. (Toledo-Arana et al., 2009). Three different promoters have been identified for the *sigC* operon (Zhang et al., 2005).

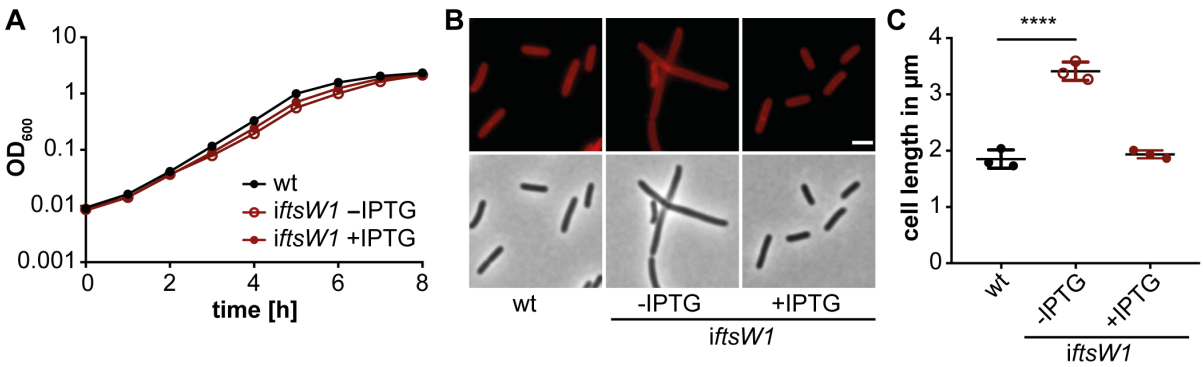

Figure 2: Depletion of FtsW1 results in cell elongation. (A) Growth of the *L. monocytogenes* FtsW1 depletion strain. Strain 10403SΔ*ftsW1* i*ftsW1* was grown overnight in BHI medium in the presence of 1 mM IPTG. The following day, the cells were washed and used to inoculate fresh BHI medium without IPTG and incubated at 37°C for 8-10h, diluted again and grown until the next morning. The depletion culture was used to inoculate BHI medium without IPTG or with 1 mM IPTG and the growth was monitored by determining OD_{600} readings at hourly intervals. Wild type *L. monocytogenes* strain 10403S (wt) was used as control. Averages and standard deviations from three independent experiments were plotted. (B) Microscopy analysis of 10403S (wt) and the *ftsW1* depletion strain grown in the presence of absence of IPTG. For depletion of FtsW1, strain 10403SΔ*ftsW1* i*ftsW1* was grown as described in panel A. Cultures of 10403S and 10403SΔ*ftsW1* i*ftsW1* were diluted 1:100 in fresh BHI medium (with 1 mM IPTG where indicated), grown for 3 h at 37°C and the cells subsequently stained with the membrane dye nile red and analyzed by fluorescence and phase contrast microscopy. The scale bar is 2 µm. (C) Cell lengths measurement of 10403S (wt) and the *ftsW1* depletion strain. The cell length of 300 cells per strain was measured and the median cell length calculated and plotted. Three independent experiments were performed, and the average and standard deviation of the median cell length plotted. For statistical analysis, a one-way ANOVA coupled with a Dunnett's multiple comparisons test was performed (**** $p \leq 0.0001$).

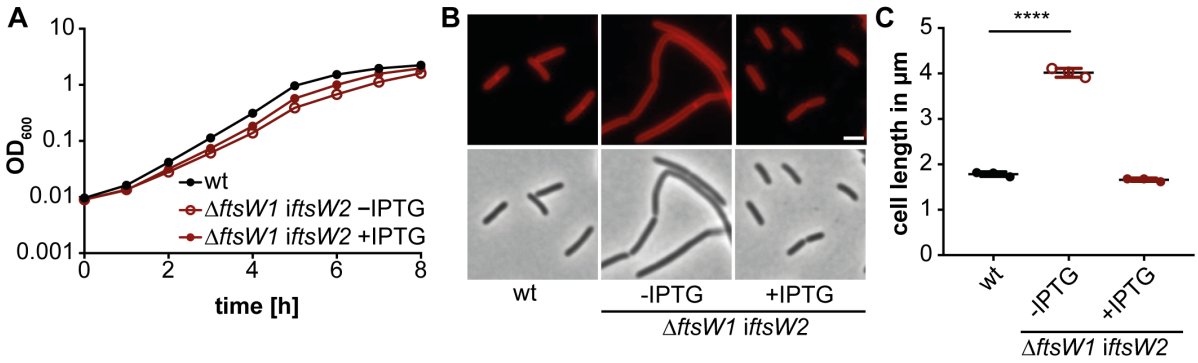

Fig. 3: Overexpression of FtsW2 can compensate for the loss of FtsW1. (A) Growth comparison of strains 10403S (wt) and 10403SΔ*ftsW1* i*ftsW2*. Growth curves were performed as described in Figure 2. (B) Microscopy images of strains 10403S (wt) and 10403SΔ*ftsW1* i*ftsW2*. For depletion of FtsW2, strain 10403SΔ*ftsW1* i*ftsW2* was grown as described in Figure 2. The next morning, cells were diluted 1:100 and grown in BHI broth (with or without IPTG as indicated) until mid-logarithmic growth phase, stained with the membrane dye nile red and subjected to fluorescence and phase contrast microscopy analysis. Scale bar is 2 µm. (C) Cell lengths measurements of 10403S (wt) and 10403SΔ*ftsW1* i*ftsW2*. The cell length of 300 cells per strain was measured and the median cell length calculated and plotted. Three independent experiments were performed, and the average and standard deviation of the median cell length plotted. For statistical analysis, a one-way ANOVA coupled with a Dunnett's multiple comparisons test was performed (**** $p \leq 0.0001$).

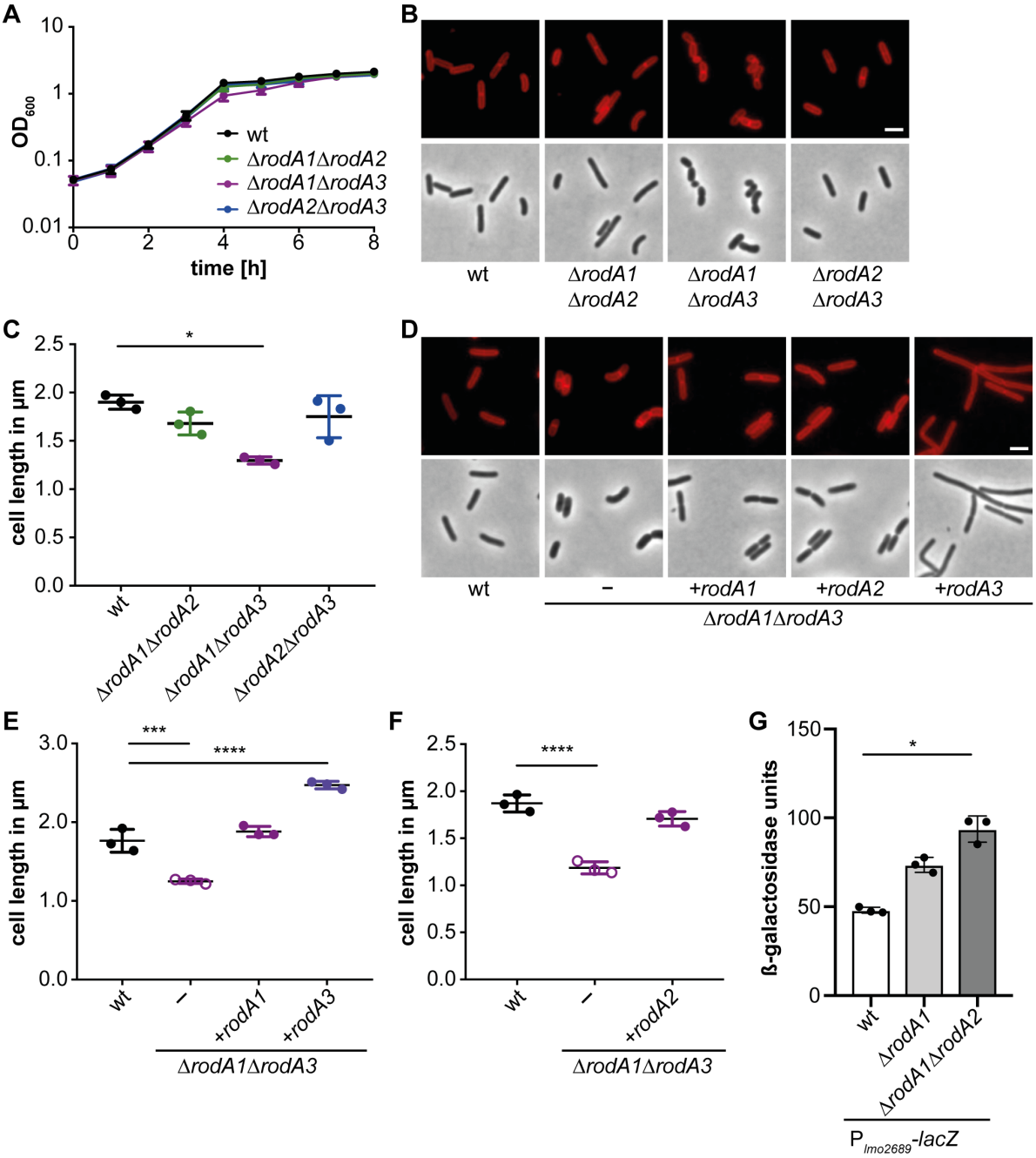

Fig. 4: RodA1 and RodA3 are essential to maintain the rod shape of *L. monocytogenes*. (A) Growth of *L. monocytogenes* 10403S (wt), 10403SΔ*rodA1*Δ*rodA2*, 10403SΔ*rodA1*Δ*rodA3* and 10403SΔ*rodA2*Δ*rodA3* strains in BHI broth at 37°C. (B) Microscopy images of wt and mutant *L. monocytogenes* strains. Cells from the strains described in panel A were stained with the membrane dye nile red and analyzed by fluorescence and phase contrast microscopy. Scale bar is 2 µm. (C) Cell lengths measurements of wt and mutant *L. monocytogenes* strains. The cell length of 300 cells per

strain was measured and the median cell length calculated and plotted. Three independent experiments were performed, and the average and standard deviation of the median cell length plotted. For statistical analysis, one-way ANOVA t-tests for multiple comparisons were used (** $p \leq 0.01$). (D) Microscopy images of wildtype and mutant *L. monocytogenes* strains. Cells from 10403S (wt), 10403SΔ*rodA1*Δ*rodA3* and 10403SΔ*rodA1*Δ*rodA3* expressing *rodA1*, *rodA2* or *rodA3* from an IPTG-inducible promoter were stained with the membrane dye nile red and analyzed by fluorescence and phase contrast microscopy. Scale bar is 2 µm. (E-F) Cell length analysis of 10403SΔ*rodA1*Δ*rodA3* complementation strains. Analysis was performed as described in panel C. (G) β-galactosidase assay using *L. monocytogenes* strains 10403S (wt), 10403SΔ*rodA1* and 10403SΔ*rodA1-2* carrying a $P_{lmo2689}$-*lacZ* fusion construct. Averages and standard deviations of three independent experiments were plotted. For statistical analysis, a one-way ANOVA coupled with a Dunnett's multiple comparisons test was used (* $p \leq 0.1$).

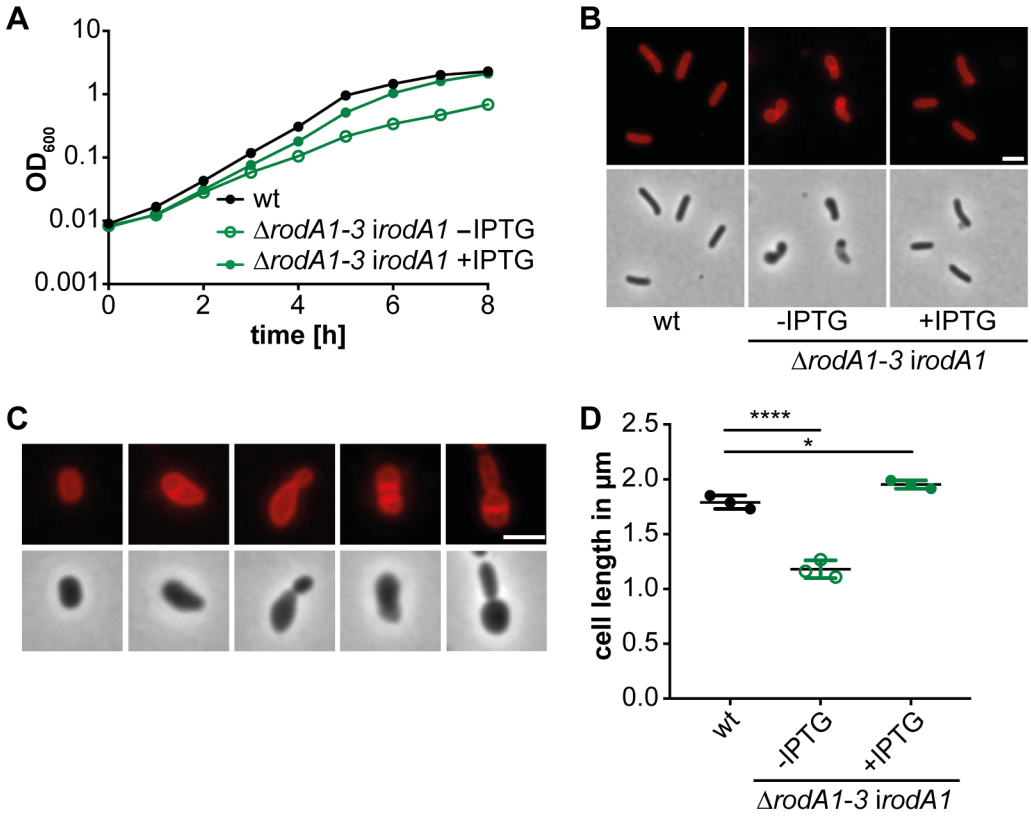

Figure 5: Absence of all three RodA proteins leads to a drastic cell shortening. (A) Growth of *L. monocytogenes* in the absence of all three RodA proteins. Growth curves were performed as described in Figure 2. (B and C) Microscopy analysis of strain 10403SΔ*rodA1-3 irodA1*. For depletion of RodA1, Strain 10403SΔ*rodA1-3 irodA1* was grown as described in Figure 2. (B) Wildtype 10403S and depleted 10403SΔ*rodA1-3 irodA1* cultures were diluted 1:100, grown for 3 h at 37°C (where indicated in the presence of 1 mM IPTG), stained with nile red and phase contrast and fluorescence microscopy images were taken. Scale bar is 2 µm. (C) Microscopy images showing examples of different cell morphologies observed for strain 10403SΔ*rodA1-3 irodA1* depleted for RodA1. Scale bar is 2 µm. (D) Cell lengths measurements of 10403S (wt) and strain 10403SΔ*rodA1-3 irodA1*. The cell length of 300 cells per strain was measured. Three independent experiments were performed, and the average and standard deviation of the median cell length plotted. For statistical analysis, a one-way ANOVA coupled with a Dunnett's multiple comparisons test was performed (* $p \leq 0.1$, **** $p \leq 0.0001$).

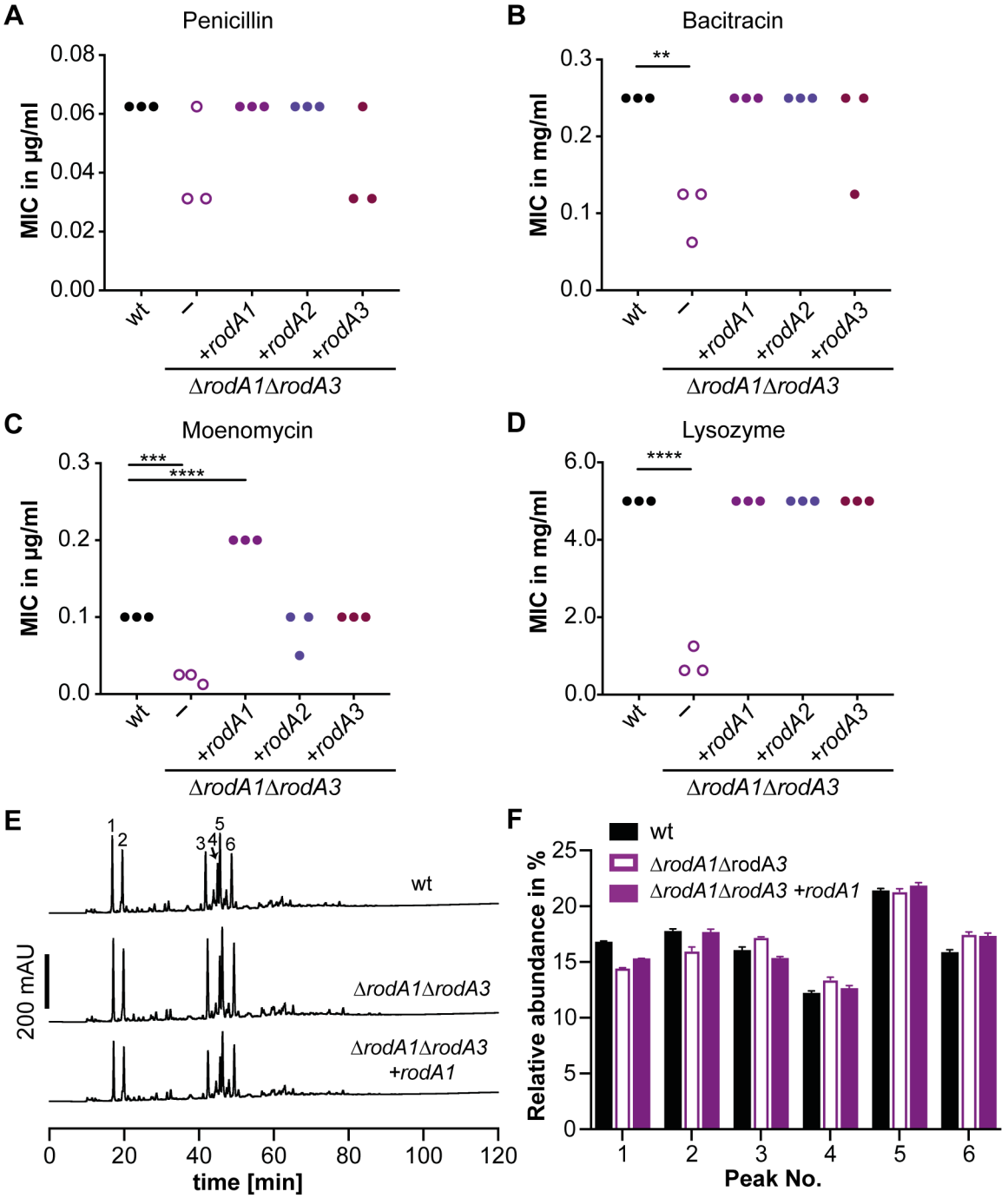

Figure 6: Impact of *rodA1* and *rodA3* deletion on the antibiotic and lysozyme resistance. The minimal inhibitory concentration for the antibiotics penicillin G (A), bacitracin A (B), moenomycin (C) and lysozyme (D) was determined for the wildtype *L. monocytogenes* strain 10403S, the Δ*rodA1*Δ*rodA3* deletion strain and the complementation strains 10403SΔ*rodA1*Δ*rodA3* i*rodA1,* 10403SΔ*rodA1*Δ*rodA3* i*rodA2* and 10403SΔ*rodA1*Δ*rodA3* i*rodA3* using a microbroth dilution assay. The complementation strains were grown in the

presence of 1 mM IPTG. The result of three biological replicates are shown in A-D. For statistical analysis, a one-way ANOVA coupled with a Dunnett's multiple comparisons test was used (** $p \leq 0.01$, *** $p \leq 0.001$, **** $p \leq 0.0001$). (E) HPLC analysis of the muropeptide composition of 10403S (wt), 10403SΔ*rodA1*Δ*rodA3* and 10403SΔ*rodA1*Δ*rodA3* i*rodA1* (grown in the presence of IPTG to induce expression of RodA1). The major muropeptide peaks are numbered 1-6 as previously described (Rismondo et al., 2015, Burke et al., 2014). (F) Relative abundance of muropeptide peaks 1-6 in peptidoglycan isolated from strains 10403S (wt), 10403SΔ*rodA1*Δ*rodA3* and 10403SΔ*rodA1*Δ*rodA3* i*rodA1*. Average values and standard deviations were calculated from three independent peptidoglycan extractions.

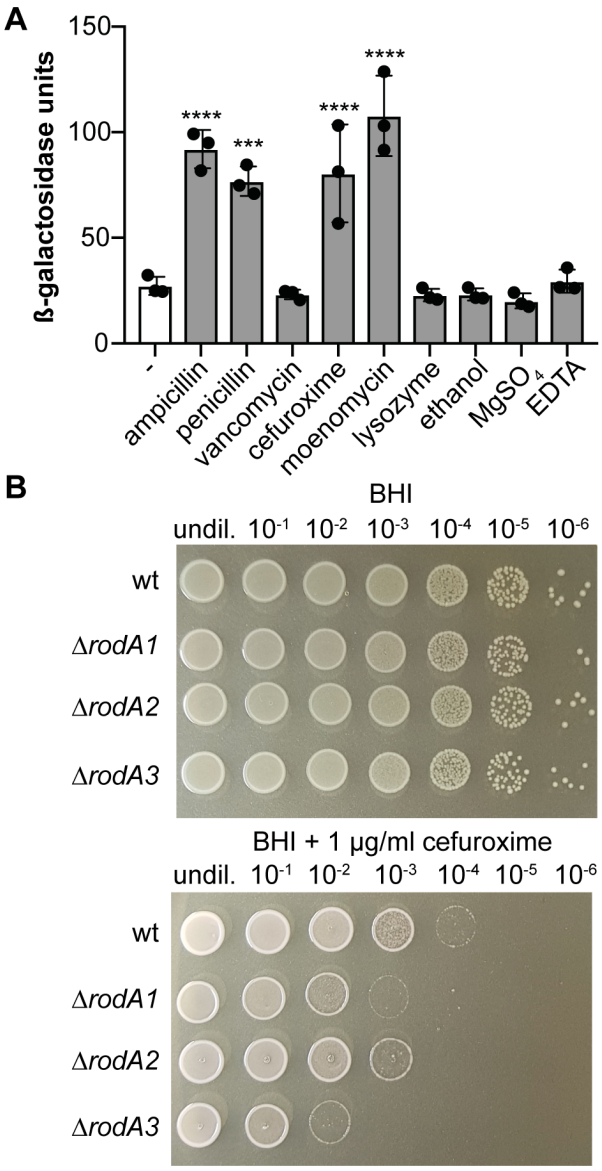

Figure 7: Cell wall-acting antibiotics increase the *lmo2689* promoter activity. (A) Bacteria from mid-logarithmic cultures of strain 10403S pPL3e-$P_{lmo2689}$-*lacZ* were exposed for 2 h at 37°C to different stressors. The activity of the *lmo2689* promoter was subsequently determined by performing β-galactosidase activity assays as described in the method section. Bacteria that had been grown in the absence of a stressor were included as negative (-) control. The averages of the β-galactosidase activity units and standard deviations from three independent experiments were plotted. For statistical analysis, a one-way ANOVA coupled with a Dunnett's multiple comparisons test was used (*** $p \leq 0.001$, **** $p \leq 0.0001$). (B) Absence of RodA3 results in decreased cefuroxime resistance. Dilutions of overnight cultures

of strains 10403S, 10403SΔ*rodA1*, 10403SΔ*rodA2* and 10403SΔ*rodA3* were spotted on BHI agar and BHI agar containing 1 µg/ml cefuroxime and incubated for 24 h at 37°C. A representative result from three independent experiments is shown.

```
Bsu RodA     ------------------------------------------------------------------MSRYKKQQSPFYQGDLIFI 19
Bsu FtsW     -------------------------------------------------------------------MLKKMLKSYDY-SLIFA 16
Lmo0421      MSSSTFEEYLGKVIANVKSKQAHSMIKKELSNHLEELSHSFQKRGLSIEDANKKAMQEMGDPSTVGRNMNQLHKPRMDW-LLIAL 84
FtsW1        -------------------------------------------------------------------MPMFKRILKSYDY-AFIAV 18
RodA1        -------------------------------------------------------------------MNQQNKLAGRIDY-GIVLS 18
RodA2        -------------------------------------------------------------------MARNRKKAVRIDY-SIIFL 18
RodA3        ---------------------------------------------------------------------------MKRDVLYN-RIILS 13
FtsW2        ---------------------------------------------------------------------------------MRAGR-VLFVT 10
                                                                                                      :.

Bsu RodA     FGVFFIISVVSIYAAGQF------GQYGNTDWIQQIVFYLLGAVAI-TVLLYFDLEQLEKLSLYIFIIGILSLIILKISPESIAP 97
Bsu FtsW     IVLLCGFGLVMVYSSSMITAVSRYGVSSNFFFMRQLFALIAGG-ALFILMALFPYKALAHQKFQKGI--LLVSVLALISLFVFGH 98
Lmo0421      FILLAGISFLPIIGD--------VVASNSSFMKKQIVWLAIAVLAL-IGFLFFDYRKLKDLWMYFYA----AALILFFTTFLVGI 156
FtsW1        FIVLCLFGLIMIYSASWSLAIG-KGLPADYFYARQVKNFIISF-IFFILFALLPFKFYQNNKVLMLI--VFGSIGVLLLIFLVGK 99
RodA1        MMLLMIISLVSIYSAQLTN-----NQYDANFVVKQAMWFVVSTFAI-IVVMQLDYDRLTKWAYYFYGL---GLFLL-VFVLLFGK 93
RodA2        MMLLCIIGLVAIYVAGLVN-----DQYTNNFLLQQSIWIVISTGVVVVIVLFFDYDKLQWAAYYLYGI---GNLLL-VLVLIVGD 94
RodA3        VFLLSLVSCVAIYFAQQT------NQYNTNFLGMQLVFLAIGTLTCF-GVSRLPIEFLRHHAIWLYVIMVITLLGI-LIPNPLVQ 90
FtsW2        YLLLAIWSLLLVYSTSYGVAVMRYKVEPSYFFNRQLLFYGLGF-LGLLVCSRINVQLFYLRRTLRIL--AGSLLGLLLLVLLTGS 92
               ::   . : :                      *      .          :                    .   .

Bsu RodA     VIKGAKSWFRIGRI-TIQPSEFMKVGLIMMLASVIGKANPKG-VRTLRDDIHLLLKIAGV---AVIPVGLILM-QDAGTAGICMF 174
Bsu FtsW     VAGNAQSWFKIGGM-SIQPGEFVKLVVILYLAAVYAKKQSYI-DHL-------LTGVAPPVVMTLIICGLIAMQPDFGTAMIIGL 174
Lmo0421      PLTGGGRWMSLWGI-AIDSPAISLFLFFIAWAGIFTKANAFKG----------WKKQVVLLIL--------FWVPVISYIIINRF 222
FtsW1        TVNNANSWLVLGPR-SLQPGEFAKLAVIIYMSAIYAKKQSYI-DDF-------NRGVLPPIFFLAFVCFLIAIQPDTGTAFIIFL 175
RodA1        EVKGAKSWIVIPFLGNIQPSEVVKVILIVVLAKVIWDHNRTYKIHRFSYDAWLLLKIGLF---TLMPLILIMLQPDLGTALVFIA 175
RodA2        ERKGSKSWISIGSLGSLQPSELMKSFLILALAKVIWDHNKKYKLHTVSLDMQLLLKIGIV---SILPLGLVALQPDLGTILVFIA 176
RodA3        NINGATRWYRFAGL-SFQPSEVVKSIFIFVLAHFAVK----Y-------QAQKWKQLGILTVLTGIVLLLIMKQPDLGTTIVYGV 163
FtsW2        AANNAQRWLSIAGV-TFQPTEMVKLLLILVIATVFLKKGCGV-RVQ-------Y----WLLGFLFLTVGLVFLQPDLGTALILGV 164
                ..  *  :     ::   .    .:.  : .  .                                          .   :

Bsu RodA     IVLVMVFMSGINWKLIAIIAGSGILLISLILLVMINFPDV----------AKSVGIQDY-QIKRVTSWVSASNETQEDSNDSWQV 250
Bsu FtsW     IATCMILCSGFSGKTLVRLVILGGIVFILVSPIIYL--------------NQDKILTEG-RLARFESLEDPFKYANS---SGLQV 241
Lmo0421      VFSIM------------------YFLCVLVMYIFYYRHNRFAIKVALGNLLVGVIFISTMILKYPSSYLPDTSIPLK-------- 281
FtsW1        VGCCIIITSGMRLRTIMKLIGIGMGIIIGLTLILFALPDS----------VRNEIVSPT-KVARITTFMNPFEYADK---EGHQL 246
RodA1        IMSGMILISGITWKIIVPLFGSIAAIGTALIWMVIYHQNW----------LTSLGFKPY-QFERITTWINPENDPQ---GGGYQV 246
RodA2        IIIGMVFISGVTWKILLPVFSSIALIGGTLIYLVMYNQEF----------LQKLGFKPY-QFKRITSWLRPEEDPL---GDGMQL 247
RodA3        TALAIILLAIKSTKLMVGIITLILTAATIGMYVVVYHISL----------LEKIGFHAY-QFSRIQTWLDPTTDPD---A-VYQL 233
FtsW2        IGVALFLTSGVGLTRLVRVAIWTFGLLLLVAMLIYFF--------------HPDFFSSA-KLGRFA-FLDPFNLDNL--DASYQL 231
                :                           :.                     .     .

Bsu RodA     DQAIMAIGSGGILGNGISNL---KVYVPESTTDFIFSIIGESFGFIGCAIVVIMFFFLIYRLVVLIDKIHPFNRFASFFCVGYTA 332
Bsu FtsW     INSYYAISSGGIFGLGLGESIQKYGYLPESHTDFIMAVIAEELGIFGVLFVIFLLGFVVIKGFYIA--RKCEDPFGSLLAIGISS 324
Lmo0421      ----DILSKAGWFGKGLHN----NLILPEAHTDFVFPFLVYSLGWVFGIFLCLLLVVFILRISRNA--FKTKDLFGRLLTIGGAV 356
FtsW1        INSFYAIGSGGVSGQGLGESVQKLGYLPEAHTDFIIAVVAEELGVFGVMFIILALFFIIFKTITTG--LRAKDPFASLMCYGIAS 329
RodA1        LRAMTAIGSGQISGNGAGYD---AIAIPENHNDFIFTIVAGDYGFIGASILLAIYFLLIYQIIRVA--LDVGVPFYSYICTGVVM 326
RodA2        LRSMQAIGSGQLQGNGIGNQ---AIAIPENHNDFIFSIIGGNFGFIGGCVLIMLYFLLIYQIIRVA--LDINIPFYSYICTGVCS 327
RodA3        NLSMKAVGSGMMTGSSGT-----NAYIPESHTDMIFSTIGHQFGFVGVSLLLILFMVLIHQLIMAA--LLMKNTFSSLVLAGFAV 311
FtsW2        RNGYYAIGSGGIFGNGLGGSIQKLGYLPEPHTDFIMTVIAEELGVFGVIWTIFLLMALSFTALYIA--ISSHFIFDSMVCIGVAS 314
                  :...   * .          :**  .*:::  :  . * .           .                *   .  *

Bsu RodA     LIVIHTFQNIGMNIGIMPVTGIPLLFVSYGGSSTLSTLIGFGIVYNASVQLTKYRSYLFNS------------------ 393
Bsu FtsW     MIAIQSFINLGGVSGLIPITGVTLPFISYGGSSLVLLLGSMGILANISMFVKYSENKKKKEPLAPKGMKKKQLKKTVYL 403
Lmo0421      LFTVPACWNILMGLGIVPIMVVPLPFISYGGSMLLVYAALLGLILNVYRRKDIVESTLVN------------------- 416
FtsW1        LIAIQAFINLGGASGLIPLTGVTLPFISYGGSSLMVLSMMLGIVANISMFTKYQRVYKADGSTK--ELPKKQKRR---- 402
RodA1        MLMFHVLENVGMNIGLLPITGIPLPFISYGGSALLGNMMAVGLVLGIRFNFKKSMFEVKEENHAS-------------- 391
RodA2        MILFHVLENIGMTIGLLPITGIPLLFVSYGGSSLLGAFMALGLVLSARYNAPEVNLGKENRF----------------- 389
RodA3        SFAFNIFENIGMTVGLMPLTGIPLPFISYGGSAVLGNFIAVGVVLAIIRSDADLIEEK--------------------- 369
FtsW2        WVSVQMFLNLGGVSGIIPLTGVPLPFISYGGSSVVMLSCAVGFVLAAARRNVL-----------------AKTREVVYL 376
              . .    *:    *::*:  : * *:*****  :     .*.:
```

Figure S1: Sequence alignment of FtsW and RodA proteins from *B. subtilis* and *L. monocytogenes*. The alignment was created using Clustal Omega (Sievers et al., 2011). Based on a study by Meeske *et al.,* amino acid residues of *B. subtilis* RodA that are essential for RodA function are colored in blue, where conservative replacements are possible in yellow and amino acids that can be changed to certain other amino acids are colored in orange (Meeske et al., 2016).

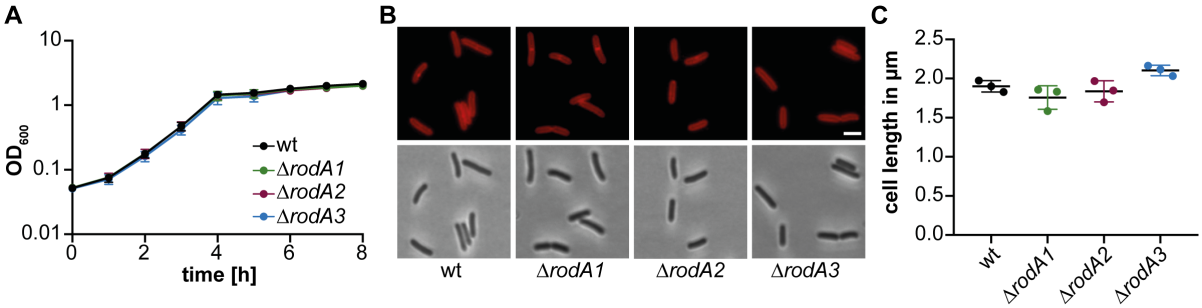

Figure S2: Single *rodA1, rodA2* or *rodA3 L. monocytogenes* strains do not show a growth or cell length defect. (A) Growth of *L. monocytogenes* 10403S (wt), 10403SΔ*rodA1*, 10403SΔ*rodA2* and 10403SΔ*rodA3* in BHI broth at 37°C. (B) Microscopy images of wildtype and mutant *L. monocytogenes* strains. Bacteria from cultures of the strains described in panel A were stained with the membrane dye nile red and analyzed by fluorescence and phase contrast microscopy. Scale bar is 2 µm. (C) Cell length of *L. monocytogenes* wt and *rodA* single mutants. The cell length of 300 cells per strain was measured and the median cell length calculated and plotted. Three independent experiments were performed, and the average and standard deviation of the median cell length plotted.

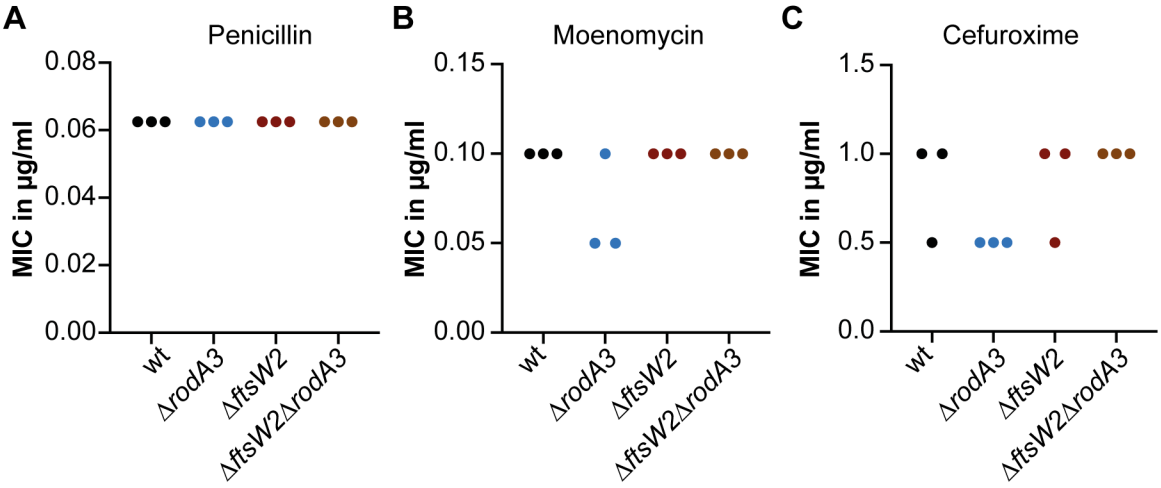

Figure S3: Deletion of *rodA3* but not *ftsW2* has a minor impact on the resistance towards a selected number of cell wall active antibiotics. The minimal inhibitory concentration for the antibiotics penicillin G (A), moenomycin (B) and cefuroxime (C) was determined for the wildtype *L. monocytogenes* strain 10403S, the 10403SΔ*rodA3* and 10403SΔ*ftsW2* single deletion strains and the 10403SΔ*ftsW2*Δ*rodA3* double mutant strain using a microbroth dilution assay. The result of three biological replicates are shown in A-C.